AGU PUBLICATIONS

JGR

Journal of Geophysical Research: Atmospheres

RESEARCH ARTICLE
10.1002/2016JD026292

Key Points:
- The multiaspect framework of heat wave and warm spells exhibits clear spatial and temporal patterns
- Most perceptible change in heat waves is observed during the post-1998 warming hiatus period, mainly exacerbated by droughts
- The 2009–2010 drought and heat wave in India can be compared with that of the 2010 Russian hot episode in terms of evolution and amplification

Correspondence to:
D. K. Panda,
dileeppanda@rediffmail.com

Citation:
Panda, D. K., A. AghaKouchak, and S. K. Ambast (2017), Increasing heat waves and warm spells in India, observed from a multiaspect framework, *J. Geophys. Res. Atmos.*, *122*, 3837–3858, doi:10.1002/2016JD026292.

Received 24 NOV 2016
Accepted 22 MAR 2017
Accepted article online 24 MAR 2017
Published online 10 APR 2017

Increasing heat waves and warm spells in India, observed from a multiaspect framework

Dileep Kumar Panda[1], Amir AghaKouchak[2], and Sunil Kumar Ambast[1]

[1]Indian Institute of Water Management, Indian Council of Agricultural Research, Bhubaneswar, Odisha, India, [2]Center for Hydrometeorology and Remote Sensing, University of California, Irvine, California, USA

Abstract Recent heat waves have been a matter of serious concern for India because of potential impacts on agriculture, food security, and socioeconomic progress. This study examines the trends and variability in frequency, duration, and intensity of hot episodes during three time periods (1951–2013, 1981–2013 and 1998–2013) by defining heat waves based on the percentile of maximum, minimum, and mean temperatures. The study also explores heat waves and their relationships with hydroclimatic variables, such as rainfall, terrestrial water storage, Palmer drought severity index, and sea surface temperature. Results reveal that the number, frequency, and duration of daytime heat waves increased considerably during the post-1980 dry and hot phase over a large area. The densely populated and agriculturally dominated northern half of India stands out as a key region where the nighttime heat wave metrics reflected the most pronounced amplifications. Despite the recent warming hiatus in India and other parts of the world, we find that both daytime and nighttime extreme measures have undergone substantial changes during or in the year following a dry year since 2002, with the probability distribution functions manifesting a hotter-than-normal climate during 1998–2013. This study shows that a few months preceding the 2010 record-breaking heat wave in Russia, India experienced the largest hot episode in the country's history. Interestingly, both these mega events are comparable in terms of their evolution and amplification. These findings emphasize the importance of planning for strategies in the context of the rising cooccurrence of dry and hot events.

Plain Language Summary Consistent with model projection and physical understanding, the multiaspect framework of heat wave and warm spells exhibits clear spatial and temporal patterns. Most perceptible change in heat waves is observed during the post-1998 warming hiatus period, mainly exacerbated by droughts. The 2009–2010 drought and heat wave in India can be compared with that of the 2010 record-breaking Russian hot episode in terms of evolution and amplification.

1. Introduction

The worldwide increase in heat waves since the beginning of the 21th century can be considered one of the most serious climate-related risks to humanity. In terms of human mortality alone, the 2003 European and 2010 Russian heat waves stand out. However, other hot extremes have had profound adverse effects on environment, infrastructure, and other living organisms in large parts of the world [*Stott et al.*, 2004; *Andersen et al.*, 2005; *Barriopedro et al.*, 2011; *Dole et al.*, 2011; *Coumou and Rahmstorf*, 2012; *Lesk et al.*, 2016]. This not only has generated intense public debate but also has prompted continuous scientific inquiry. Previous research works in the context of the projected global warming and climate variability, ranging from the regional to global scales, suggest that the frequency and intensity of hot extremes will rise in the coming decades [*Fischer and Schär*, 2010; *Donat et al.*, 2013; *Sillmann et al.*, 2013; *Russo et al.*, 2014]. According to the Fifth Assessment Report of the Intergovernmental Panel on Climate Change [*Intergovernmental Panel on Climate Change (IPCC)*, 2013], south Asian countries, accounting for about one fifth of the world's population, will be at the greatest risk in the emerging heat waves.

Most of the more than 1.25 billion people living on the Indian subcontinent are involved in outdoor activities, such as work in the agriculture and construction sectors [*Government of India*, 2013]. As a result, heat waves are a major social and environmental concern [*Murari et al.*, 2015; *Panda et al.*, 2014]. In particular, the rice-wheat cropping system of north India, which ensures rural employment and the food security of the country, is at risk from heat waves and warm spells, observed in summer (March–May) and nonsummer months, respectively [*Krishna Kumar et al.*, 2011; *Lobell et al.*, 2012; *Teixeira et al.*, 2013]. The 1998 heat wave, also

observed in other parts of the world and coinciding with the major 1997–1998 El Niño event [*De and Mukhopadhyay*, 1998], was the worst in the previous 50 years. The event resulted in more than 2500 human casualties, mostly from the east coast states adjoining to the Bay of Bengal [*De et al*., 2005]. The Indian Meteorological Department (IMD) observes that five record-setting warm years have occurred since the 1998 event, and each impacted society and environment [*Met Office*, 2011; *Indian Meteorological Department (IMD)*, 2015], even it is reported that heat stress-related casualties have limited India's labor capacity [*Dunne et al*., 2013]. The latest 2015 heat wave, a cross-border episode affecting both India and Pakistan, ranks as one of the world's most deadly hot events [*NOAA*, 2015; *United Nations Economic and Social Commission for Asia and the Pacific*, 2016].

In general, the summer heat waves in India are preceded by the cooler winter season (December–February) and succeeded by the rainy monsoon season (June–September). But, severe hot spells in the warmest month of May continue to persist well into the wet season if there is a delay and/or failure of the monsoon wind that brings moisture-laden air (i.e., rainfall) to the Indian landmass [*Webster et al*., 1998]. For example, the cooccurrences of a heat episode and drought in 2002 and 2009, which resulted crop failures, terrestrial water storage (TWS) losses, electricity shortages, and ecological disturbances, exacted huge economic losses (e.g., ~1% of gross domestic product in 2002) [*Gadgil et al*., 2004; *Panda and Wahr*, 2016]. Internationally, a considerable number of studies have shown how most mega heat waves are associated in a causal relationship with droughts and moisture deficits, including the 2003 European, 2010 Russian, 2011 Texas, and 2014 California droughts and heat waves [*Fischer et al*., 2007; *Hirschi et al*., 2011; *Barriopedro et al*., 2011; *Mueller and Seneviratne*, 2012; *AghaKouchak et al*., 2014; *Hauser et al*., 2016].

Although heat waves are typically defined as a period of consecutive days where temperatures are substantially hotter than normal, there exists no universal metrics for comparative assessment of heat waves across regions and sectors [*Meehl and Tebaldi*, 2004; *Perkins and Alexander*, 2013; *Russo et al*., 2014]. It is well recognized that threshold-based indices, such as the heat wave duration index [*Frich et al*., 2002] or combined hot days and tropical nights (CHT) [*Fischer and Schär*, 2010], have limitations. They do not capture spatially diverse climate variability, particularly in countries like India where the climate is characterized by cooler Himalayan foothills and a warmer tropical coastal belt to a hotter northwest desert region. The percentile-based warm spell duration index developed by the Expert Team on Climate Change Detection and Indices (ETCCDI), which defines a heat wave if the daytime maximum temperature (T_{max}) exceeds the 90th percentile for six consecutive days, has been effective for comparing heat wave duration for some regions [*Alexander et al*., 2006]. However, this index is not as efficient in countries like India and Australia, where the likelihood of spells of six consecutive days is rather small [*Panda et al*., 2014; *Perkins and Alexander*, 2013], yet where heat waves cause significant damage and health issues. A heat wave in India generally continues for 5 to 6 days, while most of the severe heat waves have shorter duration [*Chaudhury et al*., 2000]. A deadly heat wave may not necessarily be a prolonged one impacting hydrology and agriculture, highlighting the importance of developing sector-driven heat wave metrics.

Given the potential impacts of the current and projected increases in droughts and heat waves, with lengthening of summer-like conditions as the world warms from greenhouses gases [*Hansen et al*., 2012; *Lewis and Karoly*, 2013; *Mazdiyasni and AghaKouchak*, 2015], it is critical to improve our understanding of heat waves at regional scales. This effort is particularly essential for India, which relies so heavily on agriculture and is the world's third largest emitter of greenhouse gases, preceded by China and the USA. Using a multiaspect framework, *Fischer and Schär* [2010] first quantified changes in European heat wave characteristics, while *Perkins and Alexander* [2013] extended these aspects to assess the Australian heat waves. *Perkins et al*. [2012] have drawn global conclusions regarding the observed changes in heat waves and warm spells, emphasizing the importance of undertaking studies using a consistent framework in regions that were not part of their analysis due to sparse data coverage, such as India, Africa, and South America.

This study aims to describe the climatology, diagnostic behavior in extreme years, and assess long-term changes to heat wave and warm spell characteristics in India. To this end, a high-resolution temperature data set is utilized to assess whether there is any noticeable change during 1951–2013 and also during two subperiods (i.e., 1981–2013 and 1998–2013). Similar to *Perkins and Alexander* [2013], five aspects of heat waves are examined at the annual scale by defining heat wave as at least three consecutive days exceeding the 90th percentile of maximum temperature (TX90p), minimum temperature (TN90p), and mean temperature

(T_{mean}) (i.e., excess heat factor (EHF)). It is of vital societal interest to understand how various contributing factors influence the spatiotemporal evolution of hot episodes. We therefore examine the hydroclimatic relationships of a suite of variables, such as T_{max}, T_{min}, T_{mean}, rainfall, terrestrial water storage (TWS), self-calibrating Palmer drought severity index (PDSI), and sea surface temperature (SST) over Indian Ocean (SST-IO).

As reported in different parts of the world [e.g., *Mueller and Seneviratne*, 2012; *Diffenbaugh et al*., 2015; *Lesk et al*., 2016], a combination of hot and dry events (i.e., hotter droughts) can exacerbate human and ecosystem impacts, even far exceeding their independent signatures. Previous research has highlighted the role of atmospheric and oceanic conditions, such as blocking anticyclones and large-scale climate modes, on the genesis and extent of heat waves in India [*De and Mukhopadhyay*, 1998; *Jenamani*, 2012; *Ratnam et al*., 2016; *Rohini et al*., 2016]. Since India is a global hot spot for strong soil moisture-temperature coupling [*Miralles et al*., 2012; *Berg et al*., 2015], it is essential to understand the antecedent effect of dryness to improve the predictability of heat extremes, as more such events are anticipated in a warming climate [*Lewis and Karoly*, 2013; *Trenberth et al*., 2014].

We attempt to characterize the hotter drought years of 2002, 2009, and 2012 to understand the regional characteristics of heat wave and warm spells. In particular, the 2009 monsoon rainfall deficit was one of the most severe events on record [*Neena et al*., 2011], and the subsequent 2010 summer was an unusually intense hot season. This study provides, for the first time to our knowledge, a comprehensive description of the antecedent dry year's effects on the 2010 summertime hot extremes, akin to the July–August 2010 Russian dry-hot event [*Barriopedro et al*., 2011; *Hauser et al*., 2016].

2. Materials and Methods

2.1. Heat Wave Metrics

Using the recently developed daily gridded maximum (T_{max}) and minimum temperatures (T_{min}) for 1951–2013 with a latitude-longitude resolution of 1°×1° by IMD [*Srivastava et al*., 2009], we calculate the annual-scale multiaspect heat wave indices for the spatially uniform 329 grid points. Although summertime (March–May) heat waves cause human health hazards, primarily, the observed summer-like hot spells in nonsummer months, mostly in failed-monsoon rainfall years, can be captured in the annual scale analysis, so that potential impacts on other sectors can be evaluated. The terminology "heat wave" in this study includes both the summer season hot spells and the nonsummer warm spells. To account for the seasonal cycle, however, the daytime and nighttime heat wave thresholds are computed at each grid point by using a centered 15 day long time window as TX90p (TN90p), representing each calendar day 90th percentile of T_{max} (T_{min}), with the moving window centered on the day in question. So each calendar day of the considered study periods will have a different least-biased threshold, because they are derived from an optimum sample size.

This methodology is consistent with that of *Fischer and Schär* [2010], *Perkins et al*., [2012], and *Perkins and Alexander* [2013], so that global comparisons can be made. Using the 1961–1990 baseline period for percentile calculation, separate analysis has been carried out for the whole study period, representing the second half of the twentieth century, and that of the 1981–2013 period to depict the post-1980 rapid warming and drying phase observed in India and other parts of the world [*Hansen et al*., 2012; *Singh et al*., 2014]. Moreover, the 1998–2013 period changes are discussed in order to understand the Indian scenario during the global hiatus period [*IPCC*, 2013; *Trenberth*, 2015].

Unlike the European or ETCCDI heat wave definition, which requires at least six consecutive hot days above a threshold [*Fischer and Schär*, 2010], a minimum of three consecutive days is appropriate for the Indian climate [*Chaudhury et al*., 2000]. Moreover, as *Russo et al*. [2014] point out, this will capture 6 day duration hot spells as well. The excess heat factor (EHF) index, based on a 3 day averaged daily mean temperature, considers two excess heat indices (EHIs) to calculate the *i*th day EHF [*Nairn and Fawcett*, 2014] as $EHI_{sig} \times \max(1, EHI_{accl})$, where $EHI_{sig} = (T_i + T_{i+1} + T_{i+2})/3 - T_{95}$ and $EHI_{accl} = (T_i + T_{i+1} + T_{i+2})/3 - (T_{i-1} + \ldots + T_{i-30})/30$. Here T_i is average daily temperature for day i (i.e., average of T_{max} and T_{min} on a 24 h cycle), while T_{95} is the climatological 95th percentile of the considered time period. EHI_{sig} measures the anomaly over a 3 day window mean temperature with respect to the extreme threshold (T_{95}) for each grid point, while EHI_{accl} explains the same

window's anomaly from the preceding 30 day window. If EHF is positive for three consecutive days then there exists a heat wave-like condition. The multiplicative EHF index itself suggests a $°C^2$ unit.

For each of the percentile-based heat wave definitions described above (i.e., TX90p, TN90p, and EHF), the five aspects on an annual (January–December) scale examined here are heat wave number (HWN, events), heat wave duration (HWD, days), heat wave frequency (HWF, days), heat wave amplitude (HWA, °C), and heat wave magnitude (HWM, °C). While HWN represents the total number of heat wave events in a year satisfying the three consecutive days criteria, the length of the longest annual event is identified by HWD, and the sum of the participating heat wave days of the year by HWF. The intensity and magnitude aspects of heat waves in each year are assessed by evaluating the hottest day of the hottest heat wave event (HWA) and the average daily magnitude of all the identified heat waves (HWM). However, the timing aspect of heat waves [*Perkins et al*., 2015], which generally commence in the summer season in India, is beyond the scope of this study.

2.2. Statistical Tests

As observed by *Perkins and Alexander* [2013], heat wave metrics generally do not follow a normal distribution, because they represent the extreme states of temperature. Under ideal conditions, there is possibility of a nonoccurrence of a single heat wave, though several heat waves of extended periods have been reported in some century-scale hot years, for example, in 1998 and 2002. Thus, the nonparametric Mann-Kendall (MK) test [*Sneyers*, 1990; *Helsel and Hirsch*, 2002] is used to evaluate heat waves trends at grid scale and also for the nationally averaged time series. This robust statistical tool does not require normality of the data distribution and is also insensitive to extreme values and outliers, to which the ordinary least squares method of trend calculation is sensitive. For these advantages, the MK test has been extensively applied in a range of hydroclimatic trend detection studies [e.g., *Lettenmaier et al*., 1994; *Donat et al*., 2013; *Westra et al*., 2013]. In order to test whether a heat wave time series is statistically different from that of the null hypothesis of no trend, a two-tailed 5% level of significance (i.e., $p < 0.05$) is considered. Moreover, we calculate the magnitude of trends by using the Theil-Sen method [*Theil*, 1950; *Sen*, 1968], which is a robust nonparametic tool to more accurately estimate the rate of changes in skewed or heteroscedastic data [*Wilcox*, 2001]. For mapping the trends and understanding the spatial extent of heat wave occurrences, we employ the inverse distance weighting method of interpolation.

Although soil moisture is important to understand heat wave formation through land-atmosphere feedback, due to the lack of dense soil moisture observational networks in different parts of the world (including India), several studies have employed terrestrial water storage (TWS) observations to examine heat waves [*Andersen et al*., 2005; *Fischer et al*., 2007; *Hauser et al*., 2016]. We therefore consider the vertically integrated TWS solutions from the Gravity Recovery and Climate Experiment (GRACE) satellites, which measure soil moisture, surface water, groundwater, and snow (i.e., GRACE-TWS, centimeter). These satellite data, which have been used in a variety of hydrological researches [*Rodell et al*., 2009; *Thomas et al*., 2014; *Wouters et al*., 2014], enable an analysis of individual heat wave years and the relationship to drought. Although the GRACE products are available at three official centres, we use the available monthly anomalies during January 2002 to December 2015 of level 2 GRACE Release 05 (RL05) gravity field solutions processed from the University of Texas Center for Space Research, which reasonably captures the Indian hydroclimatic variability [*Chen et al*., 2014; *Panda and Wahr*, 2016]. This data set is used for the characterization and validation of mega heat waves, such as the 2003 European and 2010 Russian heat waves [*Andersen et al*., 2005; *Hauser et al*., 2016]. Additionally, we use the self-calibrating PDSI index, which is a more appropriate meteorological drought indicator considering the combined effect of rainfall, temperature, and evapotranspiration in the physical water balance model [*Dai*, 2011; *Trenberth et al*., 2014]. To explore the influence of the SST over Indian Ocean (20°S–30°N, 50°–120°E), we employ the updated version of the Extended Reconstructed Sea Surface Temperature Version 4 (ERSST.v4) [*Huang et al*., 2015].

3. Temporal and Spatial Variations in Heat Wave Aspects

3.1. Changes in Heat Wave Number, Duration, and Frequency Aspects (HWN, HWD, and HWF)

Figure 1 illustrates the trends and variability of the selected heat wave aspects, based on the percentile-based daytime (TX90p), nighttime (TN90p), and average (EHF) temperatures over all of India during 1951–2013. A statistically significant ($p < 0.05$) rising trend can be observed in the daytime heat wave number

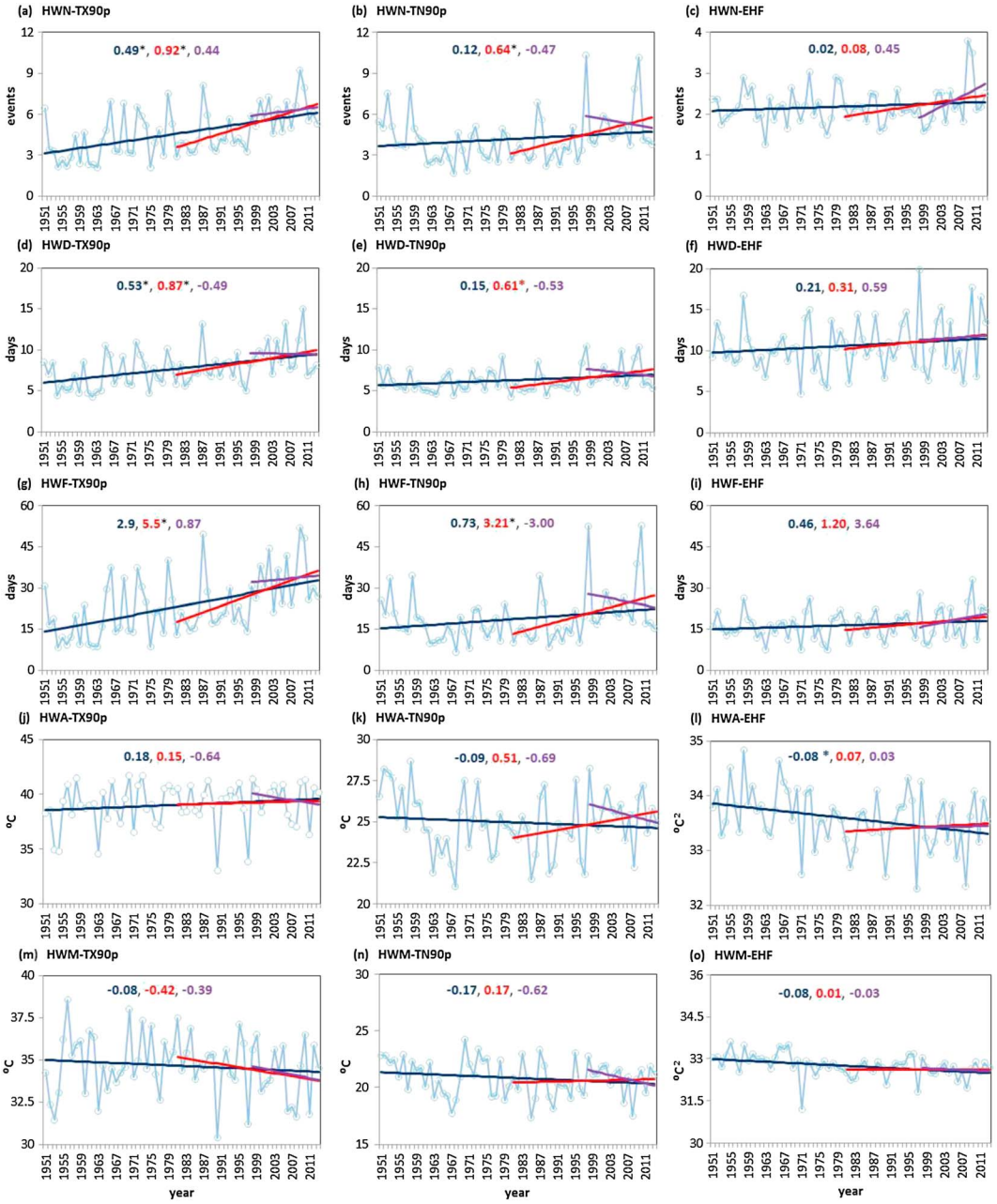

Figure 1. Averaged annual time series of heat wave metrics such as, heat wave number (HWN), duration (HWD), frequency (HWF), amplitude (HWA), and magnitude (HWM) using the percentile-based maximum (TX90p), minimum (TN90p), and average (EHF) temperatures over India. The inscribed lines denote the linear regression trend for the periods 1951–2013 (dark), 1981–2013 (red), and 1998–2013 (purple), and the corresponding Theil-Sen slope per decade (* significant at $p \leq 0.05$) is presented.

(HWN-TX90p) and the longest heat wave duration (HWD-TX90p), with the respective rates of 0.49 events per decade and 0.53 days per decade during the entire period. The corresponding nighttime indicators (i.e., HWN-TN90p and HWD-TN90p), however, display statistically insignificant changes. The daytime sum of participating heat wave days (HWF-TX90p) has increased at a faster rate of 2.9 days per decade compared to that of the nighttime sum (HWF-TN90p), though they are not statistically significant. In general, similar to the global patterns observed by *Perkins et al.* [2012], nighttime heat waves have a tendency to decline up to the mid-1960s, followed by an increasing tendency, which could be the reason for the observed insignificant trend over the entire period.

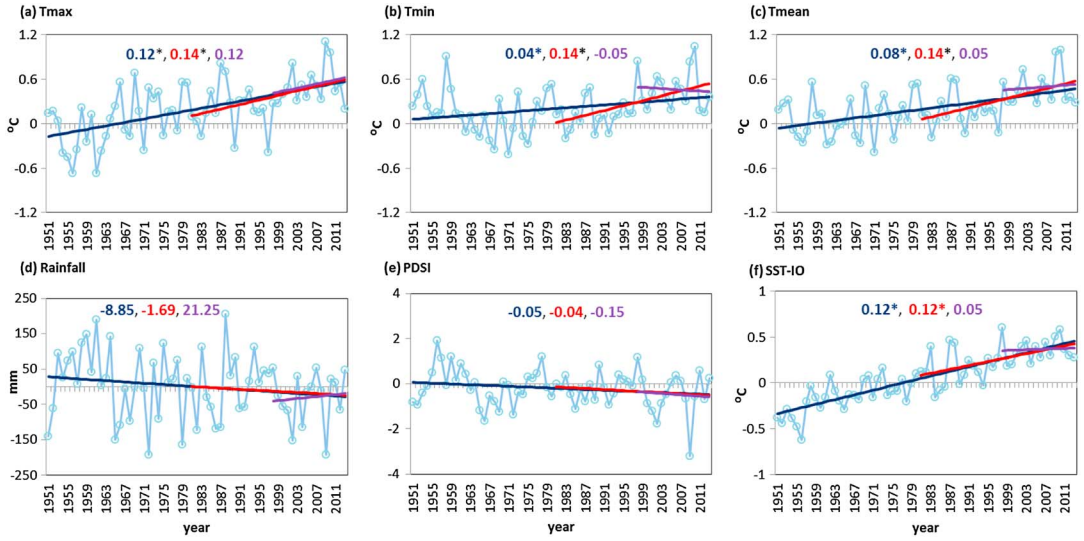

Figure 2. Averaged time series of the annual anomalies over India relative to the 1961–1990 baseline period for the daytime temperature (T_{max}), nighttime temperature (T_{min}), mean temperature (T_{mean}), rainfall, Palmer drought severity index (PDSI), and sea surface temperature over Indian Ocean (20°S–30°N, 50°–120°E; SST-IO). The inscribed lines denote the linear regression trend for the periods 1951–2013 (dark), 1981–2013 (red), and 1998–2013 (purple), and the corresponding Theil-Sen slope per decade (* significant at $p \leq 0.05$) is also presented.

It is important to note that consistent with the widely reported post-1980 faster rate of warming around the world [e.g., *Hansen et al.*, 2012; *Hoerling et al.*, 2013], the 1981–2013 period here is characterized by significant increases in the daytime and nighttime heat waves compared to the whole period (Figure 1). The occurrences and rate of change indicate that the consecutive days of extreme T_{max} of longer duration are different from that of the corresponding nighttime (T_{min}) extreme events. This differential pattern is likely to have contributed in part to the observed nondetection of trends in the T_{mean}-based EHF index, even though they support the increase in hot episodes by depicting the extreme years (e.g., 1998, 2009, and 2010) (Figures 1c, 1f, and 1i).

Similar to global patterns, the average annual T_{max}, T_{min}, and T_{mean} anomalies of the Indian subcontinent, calculated relative to the 1961–1990 baseline period, have registered a significant warming rate of 0.12, 0.04, and 0.08°C per decade, respectively, during 1951–2013 (Figures 2a–2c). Even faster is the warming rate (0.14°C per decade) during 1981–2013. In order to understand whether extreme temperatures in the form of heat waves are following a similar interannual variability as their mean states, the linear detrended time series are used to assess the relationship (i.e., correlation coefficient, r). Comparison of Figures 1 and 2 indicates that HWN-TX90p and HWF-TX90p better capture the interannual behavior of T_{max} ($r > 0.75$, $p < 0.05$) compared to HWD-TX90p ($r = 0.68$, $p < 0.05$) during 1951–2013. The corresponding nighttime hot episode's relationship with its basic data (i.e., T_{min}) is even better. However, the year-to-year variation of T_{mean} is weakly depicted in its heat wave derivatives, such as HWN-EHF ($r = 0.52$), HWD-EHF ($r = 0.40$), and HWF-EHF ($r = 0.50$), although r is statistically significant ($p < 0.05$) for a value greater than 0.24. This suggests that the daytime and nighttime heat wave aspects are generally more reflective of their respective basic time series in terms of both trend and variability.

During 1998–2013, a period reported widely in the scientific literature to represent the "pause" or "hiatus" in global warming [*Karl et al.*, 2015; *Trenberth*, 2015], trends in frequency and duration of heat waves are not statistically significant. This is not completely unprecedented in time series with large interannual variability and also presence of record-breaking heat waves in 1998, 2009, and 2010 (Figure 1). Consistently, the annual T_{max}, T_{min}, and T_{mean} anomalies (Figures 2a–2c), with respective insignificant trends of 0.12, −0.05, and 0.05°C per decade, have experienced a similar interannual behavior. In particular, T_{max} exhibits a relatively high degree of association with HWD-TX90p ($r = 0.78$) than with HWF-TX90p ($r = 0.73$) and HWN-TX90p ($r = 0.70$). Even higher is the correspondence of HWN-TN90p and HWF-TN90p with T_{min} ($r > 0.80$). This suggests that the 198–-2013 period basic (i.e., mean states) and extreme measure of temperatures have cooccurred to a

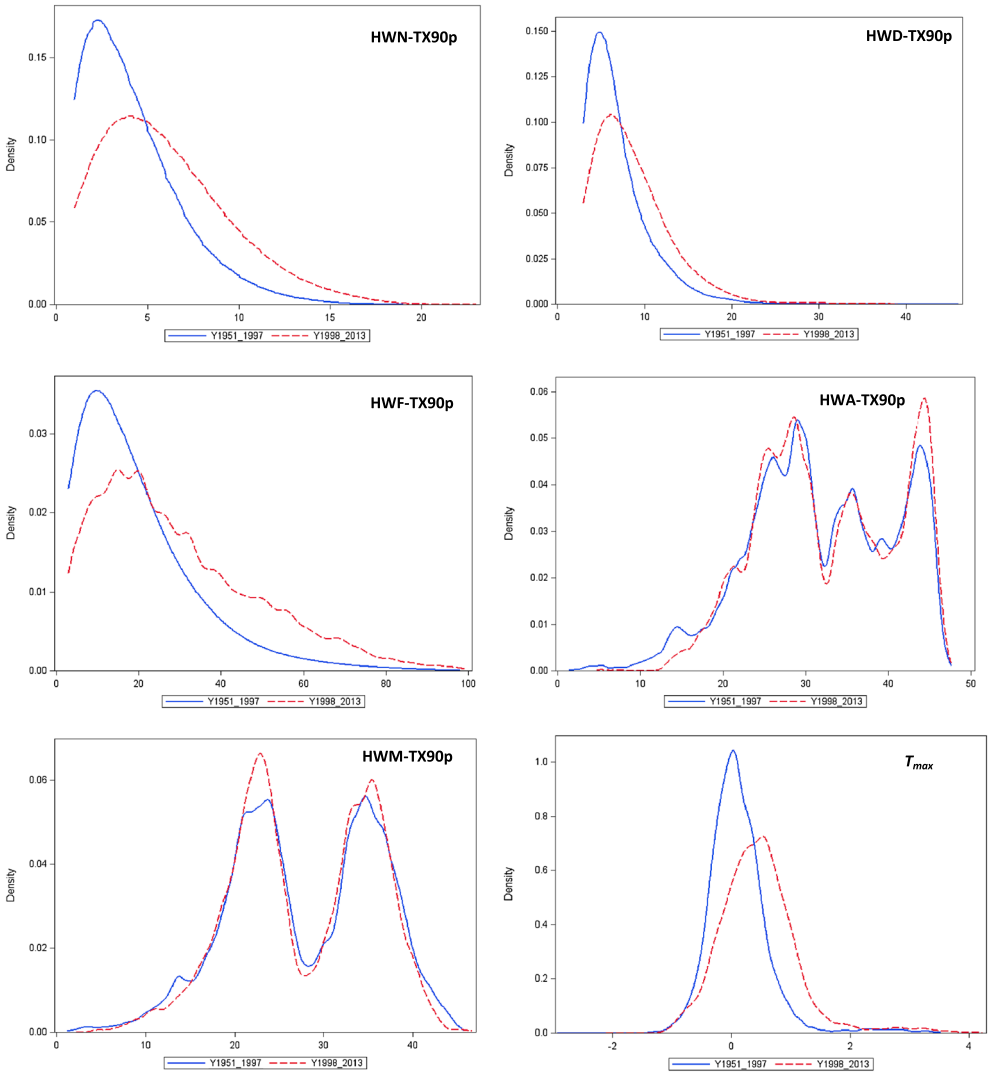

Figure 3. The probability distribution functions (PDFs) of daytime heat wave aspects for two periods: the so-called prehiatus (1951–1997) and hiatus (1998–2013) periods. The PDFs are the nonparametric curve derived from the kernel density estimation procedure with a Gaussian smoother.

more reasonable extent, thereby offering the scope of predictability of heat waves as the climate warms in the future. Nevertheless, the heat wave metrics in Figure 1 appear to have shifted upward toward a hotter climate during the hiatus period, as clearly manifested in the probability distribution functions (PDFs) in Figure 3.

The HWN-TX90p climatology during 1981–2013 indicates the prevalence of 3.5–4.5 events per year over large parts of India, compared to fewer nighttime events (Figures 4a and 4d). However, their trends in Figures 4c and 4f exhibit spatially contrasting features, with HWN-TN90p showing significant increases of two events per decade over the northern half of the country, while the rise of HWN-TX90p is prominent over the southern parts, similar to the 1951–2013 period's pattern. Note that the observed trends in nighttime heat wave numbers are close to zero generally over the southern and central landmass adjoining the eastern Bay of Bengal and the western Arabian Sea. One possible explanation for this is that daytime heating trends are nullified by cooling nighttime winds from the ocean, thus highlighting the relevance of SST patterns. During daytime, it is also interesting to observe that a horizontal northern track parallel to the foothill of the Himalayas is characterized by neutral tendencies, possibly due to the dimming effect of aerosols in the

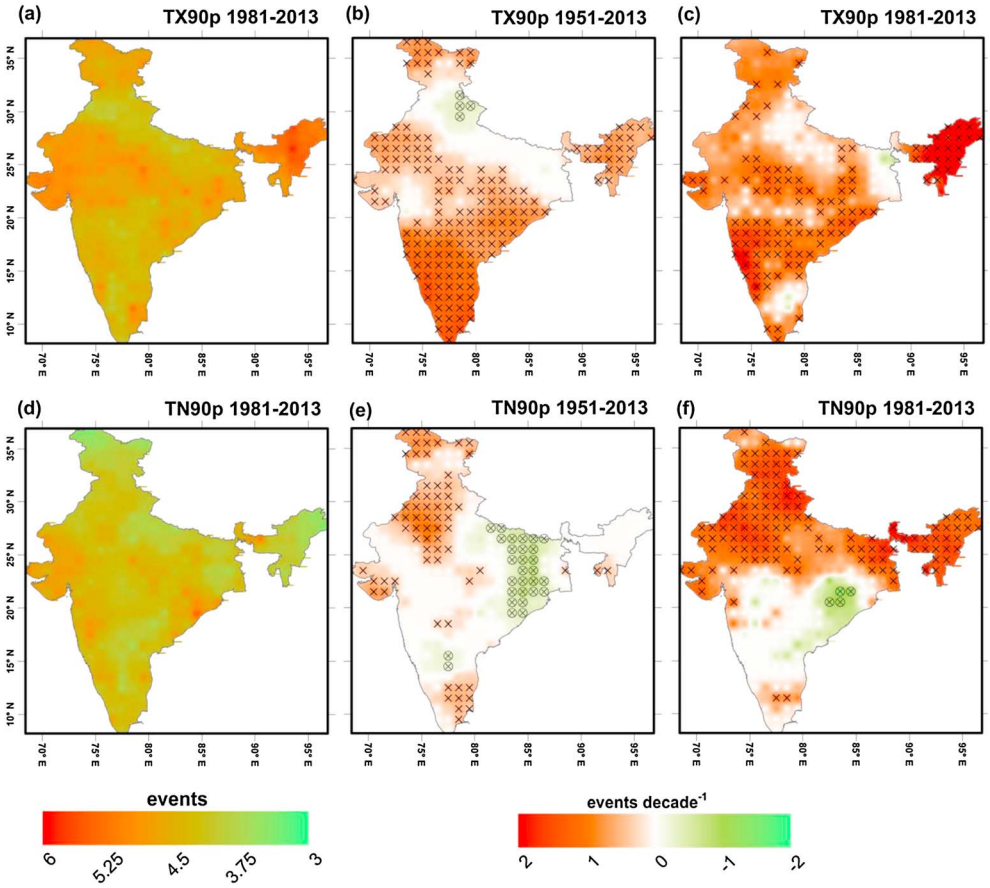

Figure 4. Spatial distribution of the 1981–2013 mean climatology for the (a) daytime (TX90p) and (d) nighttime (TN90p) heat wave number (HWN, events), (b and e) the corresponding decadal Theil-Sen trend estimates during 1951–2013, and (c and f) during 1981–2013. Statistically significant ($p < 0.05$) increasing trends are denoted by the cross symbol and that of the decreasing trends by encircled cross.

Indo-Gangetic Plains (IGP), a region well known for its vulnerability to high suspended dusts and aerosols [e.g., *Prasad and Singh*, 2007].

Comparatively, the HWD-TX90p climatology exhibits a prominent signal of hot spells (duration) of 8 to 10 days over large parts of north and central India, compared to a weak spatial distinction in HWD-TN90p (Figures 5a and 5d). Although trends in HWD are generally less significant than HWN, as also observed in the Australian climate [*Perkins and Alexander*, 2013], the 1981–2013 changes indicate that the frequently occurring nighttime heat waves over north India (Figure 4f) are also of longer duration, rising 1.5–3 days per decade (Figure 5f). This appears not to be the case for the corresponding daytime events, as evident from more areas with neutral trends (Figure 5c). The spatial congruence between the frequency-based HWN and HWF appears to be most striking, corroborated by a high temporal correlation coefficient ($r > 0.95$) irrespective of study periods and indices. Particularly, signals of the 1981–2013 hot episodes are more clearly reflected through HWF, as evident from the rising daytime heat waves of up to 8 days per decade over a large spatial domain (Figure 6c). Thus, comparison of climatologies and trends of the above three aspects of heat waves in Figures 4–6 suggests a qualitative similarity, but a focus on different impact sectors.

3.2. Changes in Heat Wave Amplitude and Magnitude Aspects (HWA and HWM)

Notably, unlike the frequency and duration aspects of heat waves, the nationally averaged time series of heat wave intensity, represented by the hottest day of the hottest event (HWA) and the average magnitude of all heat waves (HWM) in terms of absolute temperatures (°C), display generally a modest pattern (statistically insignificant) for both the daytime (TX90p) and nighttime (TN90p) measures (Figure 1). However, the

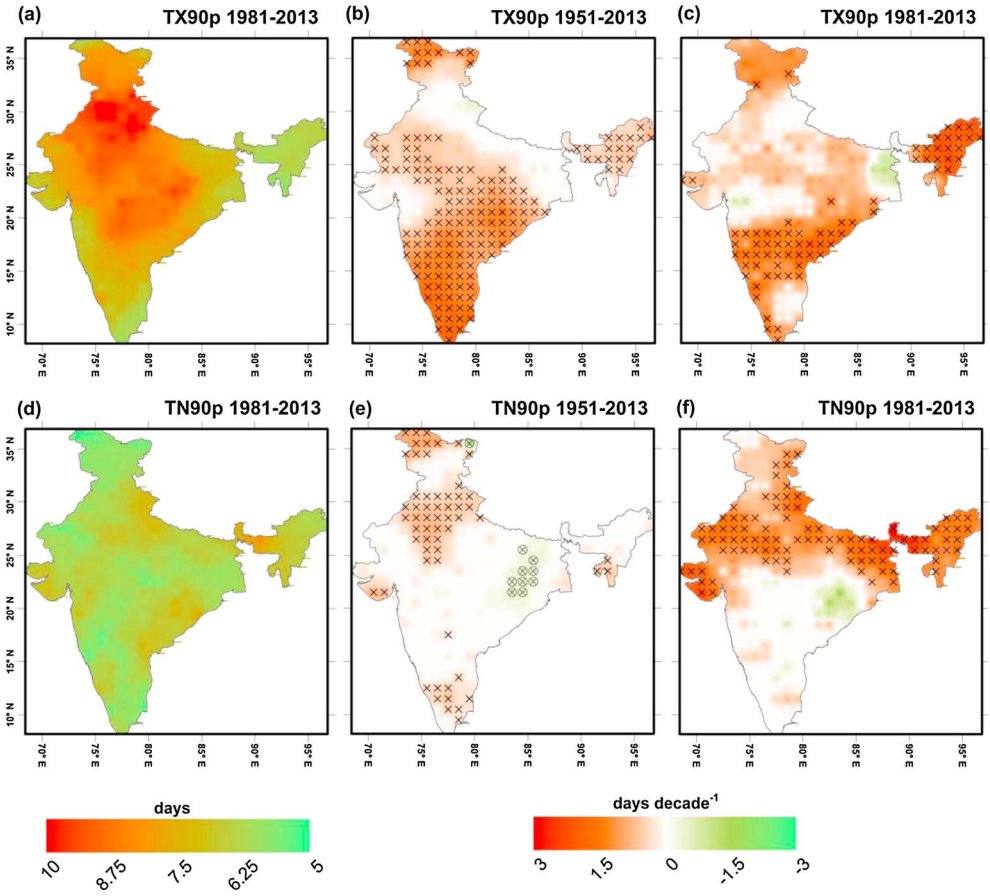

Figure 5. As in Figure 4 but for heat wave duration (HWD, days).

1981–2013 climatologies in Figures 7a and 7d reveal the large spatial extent of the hotter domain in India, with the daytime amplitude (HWA-TX90p) ranging from 40 to 45°C and the nighttime amplitude (HWA-TN90p) from 25 to 30°C, distinguishing only the cooler regions of northern and northeastern hilly ecosystem and the southwest coastal track. HWMs in Figures 8a and 8d also exhibit a similar spatial pattern, but with a different temperature range of 12 to 36°C. It is important to highlight the noticeably larger difference between the daytime and nighttime intensity, particularly the relevance of cooler nights to provide the humans and ecosystems respite from the daytime heat stress.

The nationally averaged HWA-TX90p time series is characterized by less interannual variability, increasing by 0.18°C per decade and 0.15°C per decade during 1951–2013 and 1981–2013, respectively (Figure 1j), consistent with the global average rate [*Perkins et al*., 2012]. The recent period's drop in amplitude could be attributed to switching from a significantly increasing HWA-TX90p over major areas of south and central India during 1951–2013 to neutral tendencies during 1981–2013 (Figures 7b and 7c). This change could be partly due to the post-1980 increased rate of solar radiation dimming over a large domain [*Padmakumari and Goswami*, 2010]. However, the 1981–2013 period's hottest nights (HWA-TN90p) have warmed by 0.51°C per decade (Figure 1k), particularly because of warming over the northern half of the country (Figure 7f). In contrast, a subtle declining tendency for the whole period can be linked to the concentration of significant cooling trends around the sub-Himalayan IGP (Figure 7e). Significant decreases in T_{mean}-based heat wave amplitude (HWA-EHF) during 1951–2013 (Figure 1l) appear to be driven by HWA-TN90p.

For the 1981–2013 daytime heat wave magnitude (HWM-TX90p), an unusually stronger declining trend of −0.42°C per decade is observed, mainly from the cooling tendencies over a large section of the country (Figure 8c). This not only contradicts the observed increases in HWA-TX90p but also that which is depicted

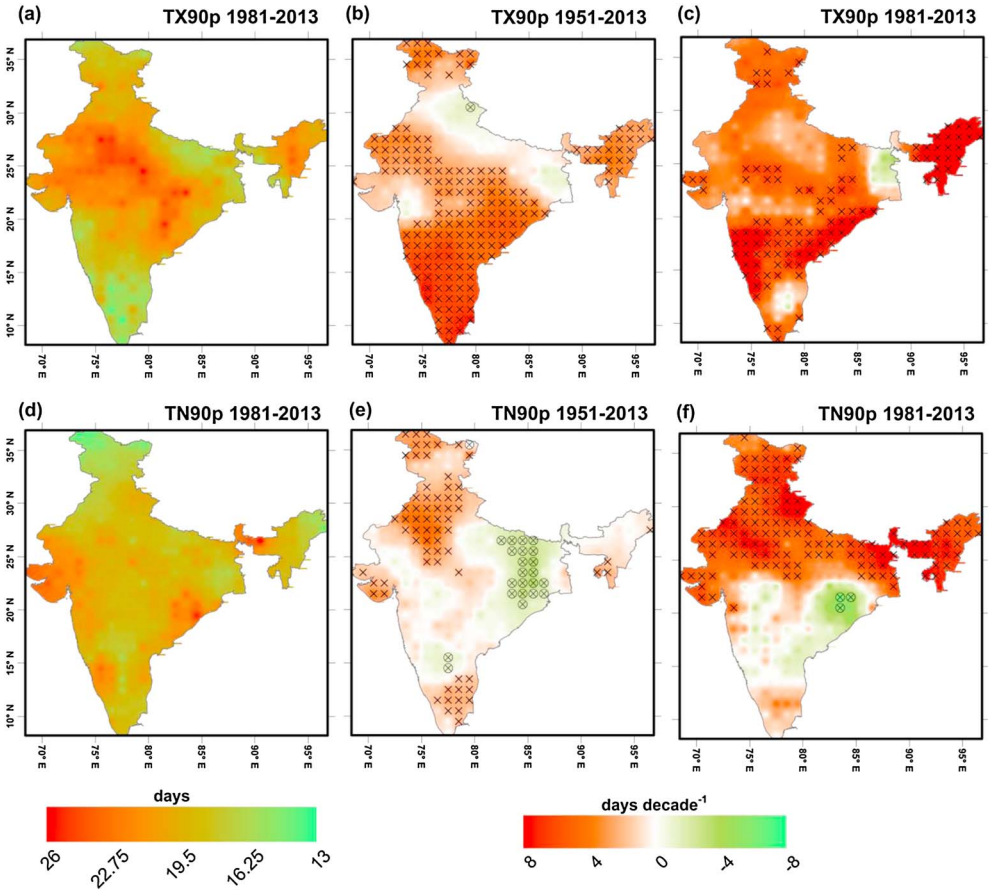

Figure 6. As in Figure 4 but for heat wave frequency (HWF, days).

in the frequency- and duration-based heat wave metrics. Even for the 1951–2013 HWA-TX90p and HWM-TX90p, the northeast part exhibits opposite trends (Figures 7b and 8b), where complex interactions of elevation, wind, cloud, and forest cover modify the heat intensity. However, the 1981–2013 nighttime heat wave magnitudes (HWM-TN90p) show a reasonable degree of temporal and spatial consistency with other metrics. Once again, the combined magnitude (HWM-EHF) has been less representative, with a low interannual variability from the mean magnitude of 33°C^2 (Figure 1o). During 1998–2013, although the nationally averaged time series shows a general decreasing pattern, both HWA-TX90p and HWA-TN90p show a warming of 0.70°C, as evident in the shift in the PDF's tails (Figure 3).

From the climate change and heat wave detection prospective, a more prominent signal manifests in HWN, HWD, and HWF. In particular, we find that HWF generates the most robust pattern, followed by HWN, even though it is difficult to determine whether the cumulative change reflected in HWF is due to HWN and/or HWD. This is consistent with the observations noted earlier by *Lau and Nath* [2012] and *Perkins and Alexander* [2013] for the North America and Australian heat wave aspects, respectively. Nevertheless, it is important to understand the physical relevance of heat wave intensity (HWA and HWM), although their trends are not statistically significant. Even a small increase in amplitude, when the atmospheric humidity is high, can increase stress levels in human beings and other organisms [*Fischer and Schär*, 2010].

4. Concurrence of Droughts and Heat Waves

At both regional and global scales, studies have reported coupling between precipitation deficits and subsequent hot extremes, particularly the role that soil dryness plays in inducing severe heat waves [e.g., *Fischer et al.*, 2007; *Hirschi et al.*, 2011; *Mueller and Seneviratne*, 2012; *Miralles et al.*, 2014; *Hauser et al.*, 2016]. We also find that the nationally averaged annual rainfall anomaly has decreased by 8.85 mm per decade

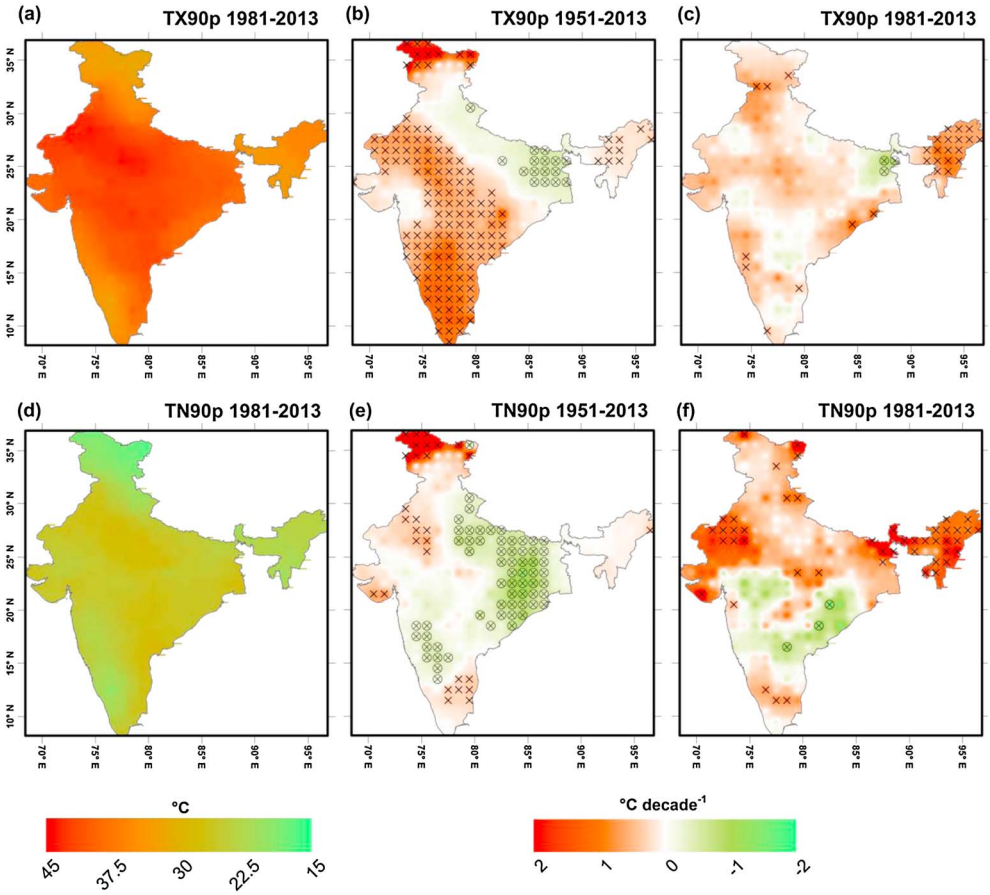

Figure 7. As in Figure 4 but for heat wave amplitude (HWA, °C).

during 1951–2013 (Figure 2d), in conjunction with the observed rises of heat wave metrics in Figure 1. This is consistent with the mechanism that dry soil tends to intensify surface warming [e.g., *Fischer et al*., 2007]. The declining PDSI index in Figure 2e, which accounts for both temperature and precipitation to better capture aridity, provides further evidence. Notably, both the rainfall and PDSI time series exhibit a prominent below-average departure (Figures 2d and 2e), consistent with the post-1980 frequent occurrences of hot episodes and implying the initiation of the dry-hot phase from about 1980. Furthermore, a significant decrease in evapotranspiration [*Padmakumari et al*., 2013] supports this rapid heating of the near-surface atmosphere in recent decades.

The monsoon's drying trend is a well-highlighted research topic [e.g., *Panda and Kumar*, 2014; *Singh et al*., 2014], because the monsoon contributes about 80% of the annual rainfall and modulates the hydrological cycle in India. However, none of the rainfall and PDSI trends (Figures 2d and 2e) are statistically significant, possibly due to the high interannual variability of the monsoon climate. Nevertheless, most of the driest years on record are concentrated in the hiatus period, which appear to have been associated with the observed post-1998 changes in heat wave behavior. This is evident from the coincident spikes in Figure 1 and also from the PDFs shifts in Figure 3. Indeed, the rainfall and heat wave time series do not correspond on a year-to-year basis and thus yield a moderate correlation coefficient of about -0.41 ($p < 0.05$) with the daytime HWN, HWD, and HWF during 1951–2013. A slightly better relationship during the recent period implies an increased cooccurrence of the dry and hot events. The loss of linear relationship in the annual time series could be due to the carryover of drought persistence from 1 year's monsoon season to the succeeding year's summer season (March to May) up until the monsoon rainfall starts. However, anticorrelation between rainfall and temperature is a common feature of the land-atmosphere interaction. The observed range in this study is

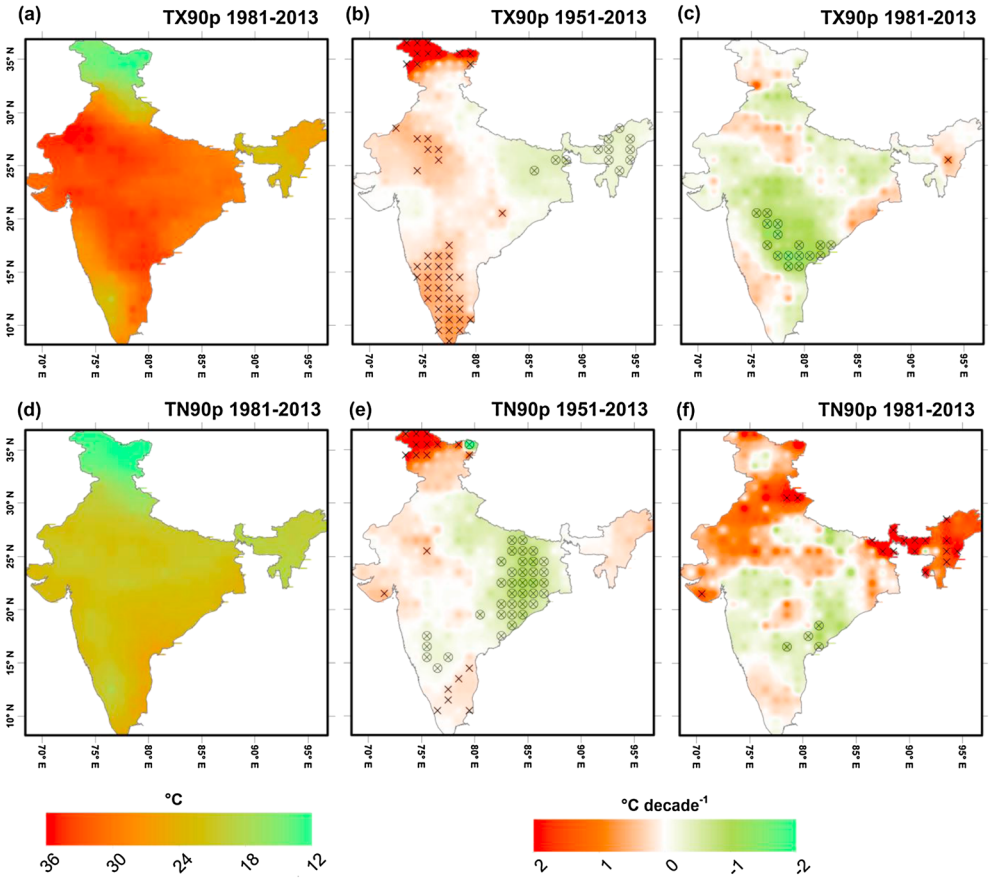

Figure 8. As in Figure 4 but for heat wave magnitude (HWM, °C).

consistent with *Berg et al*. [2015], who recognized India's higher negative correlation coefficient between the summertime T_{mean} and rainfall.

Moreover, the large-scale climatic mode that modulate of the mean and extreme metrics of temperatures is the rising SST over Indian Ocean (SST-IO) (heat waves generally occur during or succeeding El Niño events), which also induces less rainfall in India [*Panda et al*., 2014; *Roxy et al*., 2015; *Ratnam et al*., 2016; *Rohini et al*., 2016]. Therefore, it is difficult to separate the influence of the significantly warming SST-IO during 1951–2013 and 1981–2013 from that of the corresponding drying tendency (Figures 2d and 2f). However, the hiatus period nighttime hot episodes appear to be highly impacted by SST-IO, evident from a relatively stronger linkage with HWN-TN90p ($r = 0.88$), HWF-TN90p ($r = 0.76$), and HWA-TN90p ($r = 0.70$). In general, a higher correlation coefficient with T_{min} ($r = 0.66$) than with T_{max} ($r = 0.28$) suggests a differential nighttime and daytime heating in response to changes in SST-IO. Consistently, *Jenamani* [2012] observed a better relationship between the Bay of Bengal SST anomalies and minimum temperatures of the eastern coastal states of India, representing the most vulnerable region of the country since the 1998 deadly hot event. Furthermore, *Jenamani* [2012] observed that the recurving of cyclonic storms strengthen low-level westerly and thus prevent the onset of cooler sea breeze over coastal region, causing persistent heat waves. In contrast, the northcentral India heat waves are due to the anomalous quasi-stationary wave originating at the entrance of the African Jet [*Ratnam et al*., 2016].

Indeed, the most pronounced impact can be observed during the 1998 El Niño year, as the record-breaking SST-IO warming coincided with a spectacular threefold anomaly in T_{min} (0.84°C) in comparison to that of 0.27°C in T_{max} (Figures 2a, 2b, and 2f). This nighttime amplification appears to have translated into some of the record-breaking nighttime heat waves, particularly evident from the largest positive anomalies in HWN, HWD, and HWF (Figures 1b, 1e, and 1h). Nevertheless, these nighttime heat wave metrics are big enough

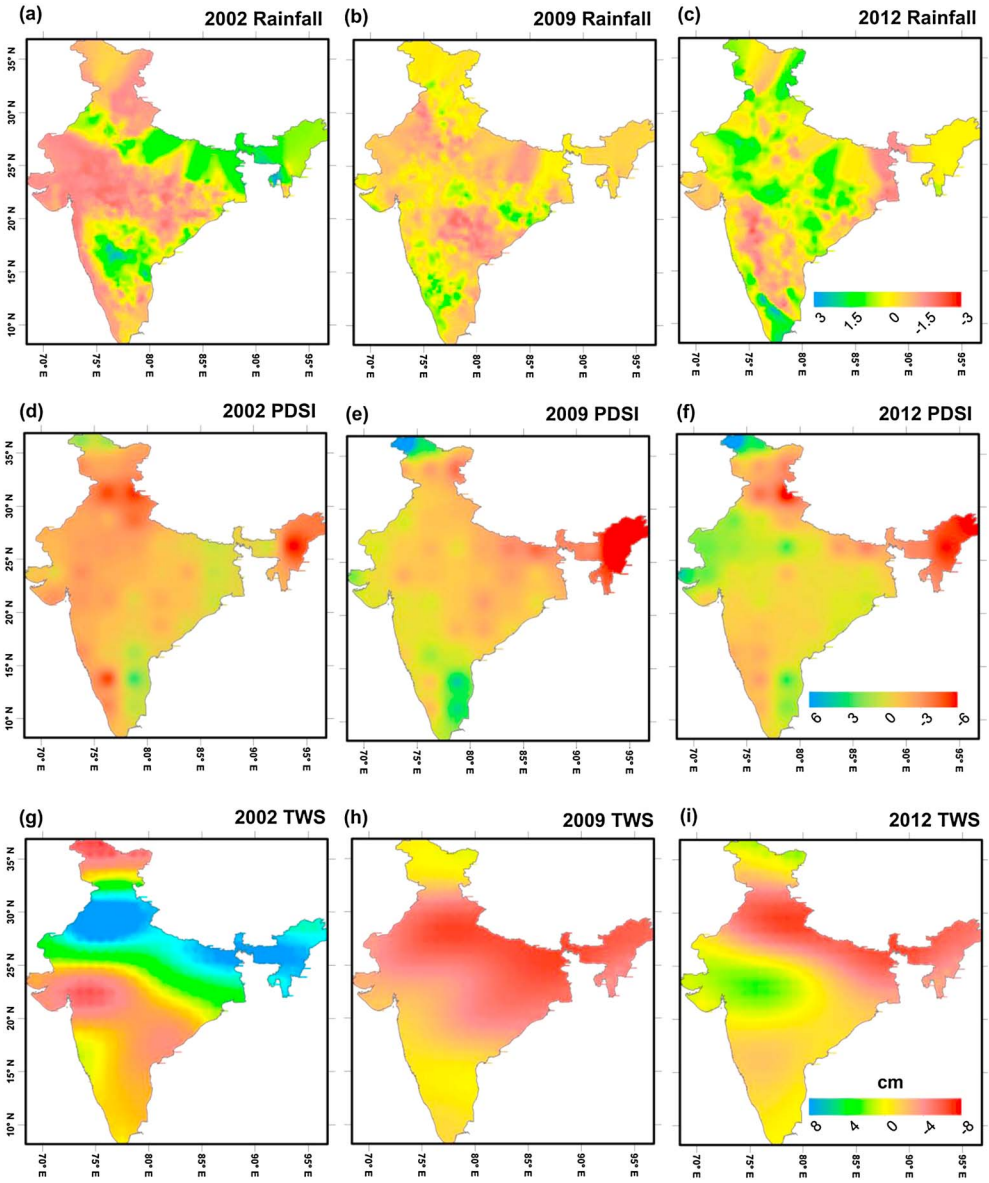

Figure 9. Spatial distribution of the anomalies of (a–c) standardized rainfall anomaly, (d–f) self-calibrating Palmer drought severity index (PDSI), and (g–i) terrestrial water storage (TWS) from GRACE for the dry years of 2002, 2009, and 2012.

to drastically alter the linear regression line by considering 1998 as the initial or the end year of analysis. The subsequent occurrence of 2009 and 2010 hot years appear to have nullified the trends.

4.1. The 2002–2003 Drought and Heat Wave

Similar to mega heat waves in other parts of the world, such as the 2003 European, 2010 Russian, and 2011 Texas heat waves [*Fischer et al*., 2007; *Barriopedro et al*., 2011; *Hoerling et al*., 2013; *Hauser et al*., 2016], most of the post-1998 heat waves in India are associated with the major droughts, particularly the century-scale droughts of 2002 and 2009, whose evolution and influence have been quite different (Figures 9 and 10). In 2002, the rainfall deficit was 56% in the active monsoon month of July, which critically affected the country's economy in terms of agricultural failure and consequent food crisis [*Bhat*, 2006]. This event was accompanied by the mean annual temperature (T_{mean}) anomaly of 0.73°C (Figure 2c), the third largest warming anomaly on record, but the SST-IO warming (0.39°C) was less noteworthy.

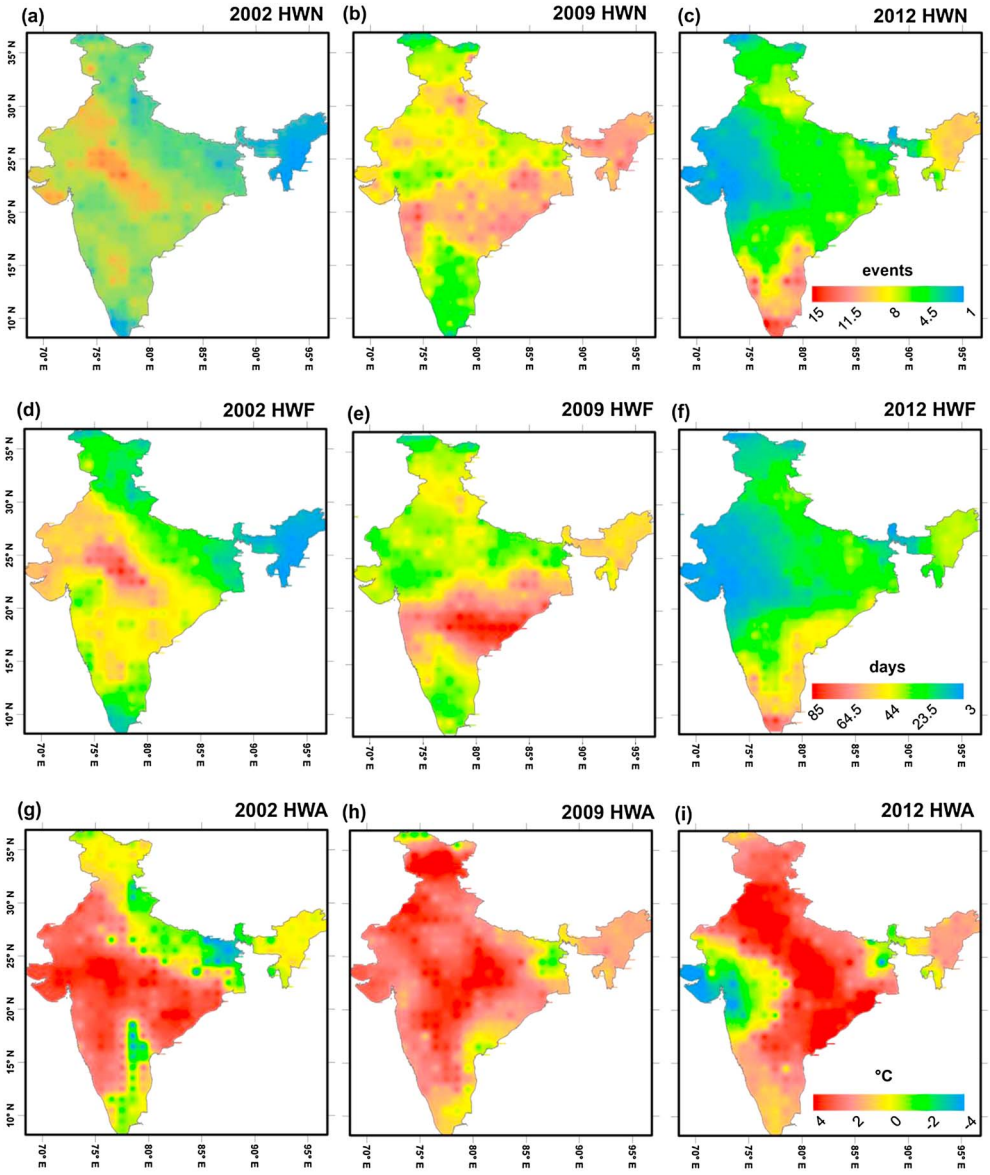

Figure 10. The corresponding spatial distribution of the daytime heat wave (a–c) number (HWN-TX90p), (d–f) frequency (HWF-TX90p), and (g–i) amplitude anomaly (HWA-TX90p) for the dry years of 2002, 2009, and 2012.

While the spatial distribution of standardized anomalies of the 2002 annual rainfall reveals major deficits exceeding 1.5 standard deviations over central and northwest India, the self-calibrating PDSI anomalies also capture the surrounding areas of moisture deficits (Figures 9a and 9d). However, the TWS anomalies from the GRACE satellites indicate a spatial inconsistency, possibly due to the bias from nonavailability of gravity records for 5 months in 2002, including the monsoon months of June and July. However, during the rest of the study period (i.e., 2003–2013), the annually averaged TWS show a reasonable correspondence with the heat wave measures, notable among them are the linear relationships (r) with HWN-TX90p (-0.58), HWF-TX90p (-0.62), and HWA-TX90p (-0.53).

Interestingly, comparison with the 2002 daytime heat wave aspects in Figure 10 indicates a reasonable spatial agreement, with HWF-TX90p and HWA-TX90p (i.e., anomalies from the 1960–1990 baseline period) more clearly capturing the domain affected by simultaneous dry and hot episodes (the diagonal strip from northwest to southeast) than HWN-TX90p do. During nighttime (not shown), some patches even

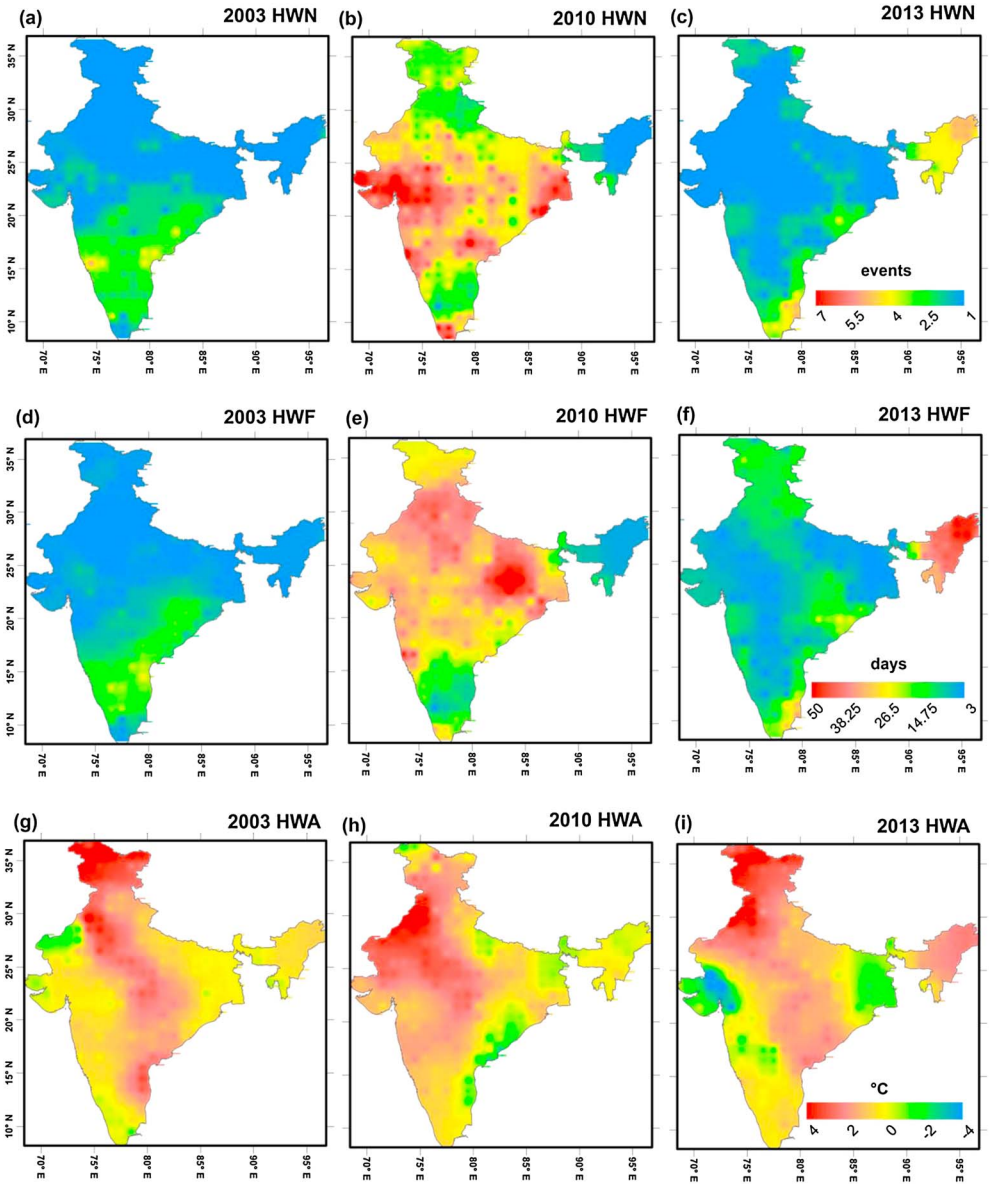

Figure 11. Summer season (i.e., March to May) daytime heat wave (a–c) number (HWN-TX90p), (d–f) frequency (HWF-TX90p), and (g–i) amplitude anomaly (HWA-TX90p) in 2003, 2010, and 2013, describing the persistence of hot episodes following the worst droughts illustrated in Figure 9. The 2010 summer season depicts the record-breaking heat waves.

experienced more heat waves. A spectacular rise of T_{max} associated with the monsoon rainfall break spell during 4–17 July 2002 over a large domain of central India [*Rajeevan et al*., 2010] supports the evolution of heat waves. To further understand the severity of antecedent soil moisture deficits on the subsequent summertime hot conditions, we plot in Figures 11 and 12 the March–May daytime and nighttime heat waves in 2003, 2010, and 2013.

The 2003 summer season shows a rise in HWN-TX90p and HWF-TX90p over the east and south (Figures 11a and 11d), but the nighttime warming is more pronounced, clearly manifested in HWN-TN90p and HWF-TN90p (Figures 12a and 12d). This explains why the 2003 summer was as deadly as 1998 [*Bhadram et al*., 2005], which also featured record-breaking nighttime amplifications (Figures 1b,1e, and 1k). Using National Centers for Environmental Prediction/National Center for Atmospheric Research (NCEP/NCAR) reanalysis data, *Jenamani* [2012] attributed the 2003 heat stress to the sea breeze cutoff from the Bay of Bengal,

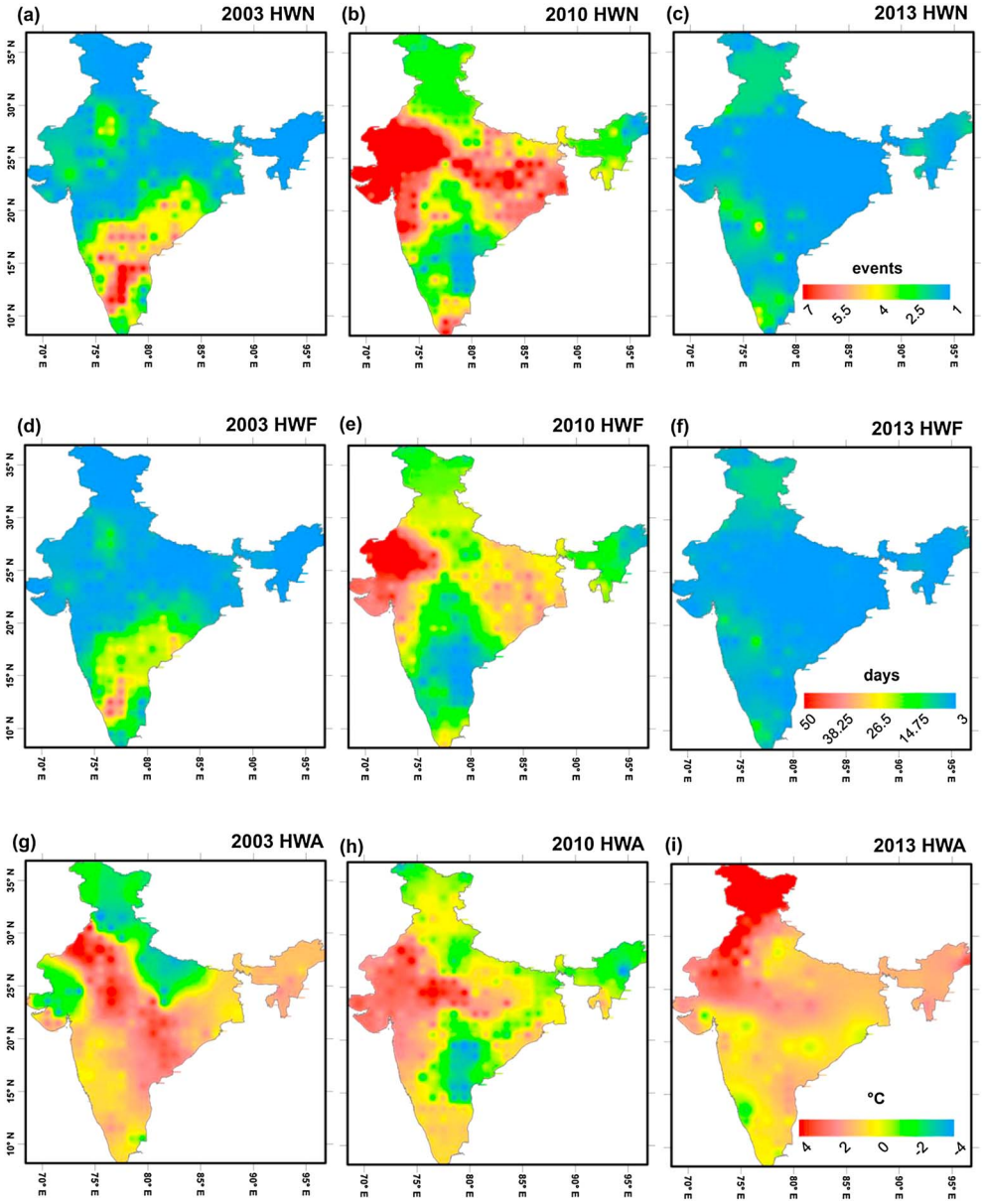

Figure 12. As in Figure 11 but for the nighttime (TN90p) heat wave metrics.

which would have subsided the daytime heat and provided nighttime relief. However, a critical look at the 2003 heat wave amplitudes indicates that the HWA-TX90p and HWA-TN90p anomalies exceeding 3 to 5°C (Figures 11g and 12g) also occurred over northcentral and east coast India, coinciding the 2002 drought prevalence. This underscores how lethal coastal humidity and wind cutoff could be, as millions of chickens also died of heat stress, a heavy blow to the poultry industry [*BBC*, 2003; *Kumari and Maiti*, 2016].

4.2. The 2009–2010 Drought and Heat Wave

The severity of the 2009 drought and heat wave was primarily due to the 47% rainfall deficit in June [*Samanta et al.*, 2015], as June rainfall dissipates the previous months' hot spells and initiates the wet monsoon season. This carry-over of high summer temperatures appeared to be further amplified with another monsoon break in July, thus creating the most extreme dry-hot event in the country's history. The signature of this event is apparent from rainfall deficits and PDSI declines over a large spatial extent (Figures 9b and 9e), while the annual rainfall and PDSI anomalies reached a record low value, accompanied by the largest daytime

warming (T_{max}) of 1.10°C (Figures 2a, 2d, and 2e). Moreover, the water storage losses captured by TWS, showing a uniform declining pattern over north and northeast India (Figure 9h), point to the indirect effect of climate as a consequence of excess anthropogenic groundwater withdrawal to meet the drought and heat stress-induced irrigation requirements of the predominant rice-wheat cropping system [*Panda and Wahr*, 2016]. It is worth stating that the 2009 dry-hot year caused the largest annual TWS depletion in GRACE's history until 2016, with a mean anomaly of −3.63 cm, which corresponds to more than 1.2 standard deviations.

Consistently, the spatial extension of the 2009 heat wave suggests a nationwide incidence (Figures 10b and 10e), with the daytime heat wave number and frequency (HWN-TX90p and HWF-TX90p) registering record values during the study period (Figures 1b and 1h). The HWA-TX90p anomaly also shows a large-scale rise of about 1 to 4°C (Figure 10h). The origin of this mega event could even be traced back to the 2008 moisture deficits, as anticyclonic circulation anomalies over the Bay of Bengal and central India resulted in a below-normal rainfall [*Rao et al*., 2010], with consequent TWS depletions [*Panda and Wahr*, 2016]. Added to this was the incursion of dry desert air associated with the blocking high over the Arabian Peninsula during the 2009 summer season, which caused the long break in June 2009 by inhibiting the growth of deep convection over central India [*Krishnamurti et al*., 2010]. All together these events appear to have initiated the 2009 heat waves. The subsequent reduction in soil moisture and TWS corroborates the amplification of the 2009 hot episodes through land-atmosphere feedbacks, which have been demonstrated as key to most of the mega heat waves around the world [e.g., *Miralles et al*., 2014; *Hauser et al*., 2016].

On the contrary, equally severe hot episodes occurred in 2010 in Figure 1, despite a wet year with intense rainfall induced flooding in parts of India and Pakistan [*Lau and Kim*, 2011; *Trenberth and Fasullo*, 2012], as evident from the above-average rainfall and PDSI anomalies in Figures 1 and 2. By analyzing the summer season heat wave metrics specifically, we find that the summer 2010 contributed a large proportion and thereby modulated the annual heat wave features. This suggests that the 2009 dry-hot condition persisted the whole year and was further amplified in the 2010 dry summer season before finally reaching a peak at the onset of the monsoon rainfall. This is evident from the 2010 summertime HWD-TX90p, HWF-TX90p, and HWN-TX90p, exhibiting a more than twofold rise from that of 2009. The corresponding nighttime heat waves were even more anomalous. Nevertheless, the summertime TWS and PDSI anomalies during 2010 reflected the background drying condition of soil for enhancing sensible heat fluxes, thereby exacerbating the strength of the heat wave.

Indeed, TWS exhibited the largest soil water storage loss in summer 2010, as the mean anomaly reached −12.78 cm. And this drop could not be replenished with the subsequent above-normal monsoon rainfall, leading to the annual anomaly of −3.25 cm compared to the 2009 peak anomaly of −3.64 cm. These results are consistent with the results of *Hauser et al*. [2016], who observed a TWS anomaly of about 1 to 2 standard deviation associated with the 2010 Russian heat wave. Similarly, *Long et al*. [2013] reported the greatest TWS depletion in Texas due to the 2011 drought and heat wave. It is important to emphasize that the summer 2010 TWS loss in India reflects the signature of the 2009 monsoon drought and hot spells illustrated in Figure 9h, plus the effect of the record-breaking 2010 summer heat wave, which are difficult to separate from the current data set.

All the five aspects of the 2010 summertime heat wave exhibit large amplitudes and spatial extents (Figures 11 and 12) that appear to be outside the range of identified trends and variability. In particular, the daytime events have occurred over much of the northern and central India, depicting rationally the spatial orientation of the previous year's drought and soil water storage losses in Figure 9. This provides a robust evidence of the culmination of land-atmosphere feedback, as no anticyclonic anomalies and the associated monsoon breaks occurred in 2010 [*Samanta et al*., 2015]. Note that there is a clear difference between the spatial orientation of HWN-TX90p and HWF-TX90p (Figures 11b and 11e). This is due to the prolonged but not frequent nature of the 2010 heat wave, evident from the largest HWD-TX90p in Figure 1d.

This extended hot spell specifically in March, coinciding with the grain-filling stage of the predominant wheat crop in IGP, led to an estimated yield loss of 6%, as T_{max} exceeded the physiologically critical threshold of 40°C [*Gupta et al*., 2010; *Rao et al*., 2015]. Moreover, for the 2010 summer as a whole, severity of heat stress is evident as the frequency of T_{max} above 40°C and CHT exceeded 3 and 2.38 standard deviations, respectively. This dry-hot event impacted the food security of the country, as the total food grain production in the 2009–2010 hydrological year dropped by 16.36 million metric tons (about 8%) [*Agricultural Statistics*, 2013].

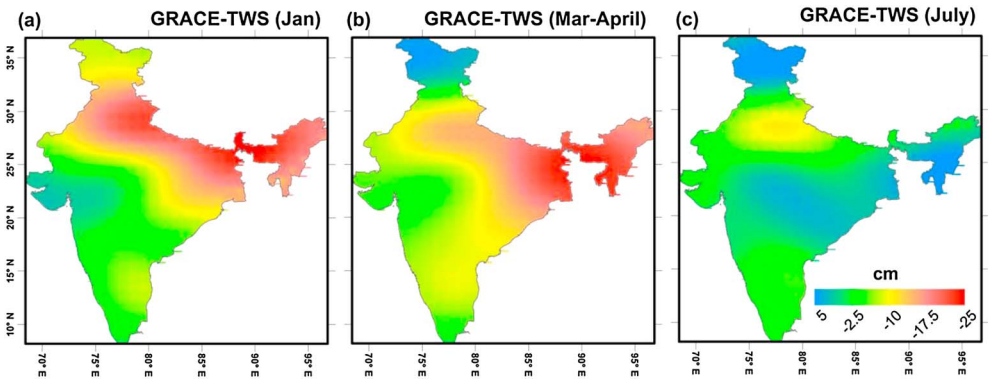

Figure 13. Spatial distribution of terrestrial water storage (TWS) anomalies from GRACE for (a) January, (b) March–April, and (c) July 2015.

However, in spite of the pronounced nighttime heat waves (Figures 12b and 12e), along with the SST-IO warming of about 0.58°C (second largest anomaly after the 1998 event), health hazard was not that serious as in 1998 and 2003, except the localized urban mortality in Ahmedabad, Northwest India [*Azhar et al*., 2014]. This highlights the affiliation of different heat wave metrics to impact sectors, as HWD causes agricultural losses, but may not induce human mortality due to the likely increase in resilience compared to abrupt heat waves.

4.3. The 2012–2013 and 2014–2015 Drought and Heat Wave

The rainfall deficits in 2012 and 2014 are not as widespread as the two previously explained droughts, but the succeeding summer seasons have been deadly, particularly over the east coast region [*IMD*, 2014; *Malini et al*., 2016]. In 2012, both rainfall and PDSI anomalies (Figures 9c and 9f) indicate prevalence of moisture-deficit conditions over south Peninsula and parts of northern and northeastern India, reasonably comparable with the heat wave (HWN-TX90p and HWF-TX90p) distribution in Figures 10c and 10f. The persistence of these dry-hot episodes can also be seen in the 2013 summertime HWN-TX90p and HWF-TX90p (Figures 11c and 11f). The corresponding nighttime events (Figures 12c and 12f) suggest that most part of the country experienced only one heat wave, but over 1000 human casualties were reported from the east coast state of Andhra Pradesh [*Malini et al*., 2016]. This was particularly due to the sudden rise in temperature to which people could not acclimatize. Consistently, both the hottest day and night temperatures (i.e., HWA-TX90p and HWA-TN90p anomalies) exhibit the warmth similar to that of the 2003 hot event (Figures 11i and 12i).

For the 2015 heat wave, although *Ratnam et al*. [2016] observed blocking anticyclones to have caused the event over northwest and central India, we argue that the strong coupling of soil water deficit and temperature [*Miralles et al*., 2012; *Ramarao et al*., 2016] is likely to have translated into hot extremes, similar to that of the 2009 event. Because this hot event was preceded by dry conditions with the monsoon and post-monsoon (October–December) rainfall deficits of about 22% and 33%, respectively in 2014 over the same region [*IMD*, 2014]. In the absence of an updated meteorological data set, TWS during January 2015, reflecting the cumulated signal of the preceding year rainfall deficits and the subsequent post-monsoon groundwater withdrawals, exhibits pronounced water storage losses particularly over the highly irrigated IGP region (Figure 13a). This has turned out to be the peak drop, as the average reached −10 cm (about 2.3 standard deviations). The March–April TWS loss (since May records are not available), of comparable magnitude to that of the 2010 worst heat wave year, shows further extension to the eastern and southeastern parts in Figure 13b. Interestingly, this spatial distribution of water storage loss corresponds reasonably with the identified region of extreme T_{max} during the 2015 summertime heat wave [*NOAA*, 2015; *Pattanaik et al*., 2016].

Moreover, it is well established that sufficient wetness of soil triggers enough evaporative cooling that even frequent anticyclones can hardly increase temperatures to produce hot days, but antecedent moisture-deficit conditions being sensitive to atmospheric circulation can induce hot extremes [*Mueller and Seneviratne*, 2012; *Quesada et al*., 2012]. Recently, *Hauser et al*. [2016] quantified that the 2010 soil moisture deficit alone contributed to a sixfold increase in risk of severe heat wave in western Russia. In India, a steady rise in rainfall failures since 1998 associated with anticyclonic Rossby wave breaking has led to moisture deficits over central and

northwest parts, with NCEP/NCAR reanalysis data showing prominent wind field patterns in 2002 and 2009 [*Samanta et al*., 2015]. The same region also shows a strong soil moisture and temperature coupling, leading to a higher surface warming during break periods [*Miralles et al*., 2012; *Ramarao et al*., 2016]. Nevertheless, our results provide evidence of an increased propensity of heat wave frequency than that of intensity due to moisture deficits for the considered dry years.

5. Summary and Conclusions

This study examines whether and to what extent heat waves and warm spells in India have changed since the mid-20th century, using a multiaspect framework to accommodate wide range of impact sectors. Consistent with the simultaneous increase in dry and hot extremes over several regions of the world [*Perkins et al*., 2012; *IPCC*, 2013], the Indian subcontinent has experienced a general rise in the frequency of heat waves. It is, however, interesting to find the distinctive spatial, temporal, and diurnal evolution of heat wave characteristics. At the global scale, *Seneviratne et al*. [2014] observed that the hot extremes continued to increase during the global warming hiatus, without any major El Niño event. Consistently, most of the subcontinent's severe heat waves occurred during 1998–2013, with a marked shift in the probability distribution functions toward warm extremes. This hotter-than-normal climate has also been accompanied by an equally anomalous drying phase, consistent with the rising post-1998 dry-hot episodes. As India is projected to be a global hot spot of heat stress on agricultural crops [*Teixeira et al*., 2013], persistence of dry-hot spells, particularly the pronounced nighttime warming causing significant rice yield reduction [*Peng et al*., 2004], could pose a risk to the country's future food security. Overall, our results show that the increasing heat wave tendency, which will likely continue because of the projected warming in the 21st century, is a daunting challenge that India faces.

Notably, our findings show that the 2009–2010 drought and heat wave in India, whose spatial extent and strength exceeded the previous records, are comparable in terms of evolution and amplification with that of the 2010 record-breaking Russian hot episode. The latter was attributed to the interaction of anticyclone circulations over western Russia and soil moisture-temperature feedback. Consistently, although the pronounced heat waves of the 2010 summer season appear to arise from the 2009 intrusion of dry air from the west Asia desert toward central India associated with blocking anticyclones, it is the antecedent drying conditions that provided the necessary amplification to produce the observed hot extremes.

Globally, the year 2010 stands out clearly in terms of extreme events, with the largest summertime warming over the Northern Hemisphere during June to August [*Hansen et al*., 2012; *Trenberth and Fasullo*, 2012]. However, India appears to differ because this period corresponds to the wet monsoon months, with a drop in temperature following heavy rainfalls over the northern parts in July 2010. Chronological occurrence of the 2010 extreme events suggests that the record-breaking warming of the north Indian Ocean in May was followed by intense rainfalls in several parts of India and China in June and July and then by the simultaneous occurrence of heavy rainfall over Pakistan and mega heat wave in Russia in July and August [*Lau and Kim*, 2011; *Trenberth and Fasullo*, 2012]. This study shows that just preceding the mega heat wave in Russia, the Indian subcontinent experienced a record-breaking combination of dry and hot events, evident from the 2010 summertime (March–May) heat wave metrics. Whether this was the precursor to the observed extremes in other neighboring regions is an important question. Therefore, future research needs to critically explore the teleconnection and feedback mechanism in a broader prospective to improve the prediction of heat waves.

Acknowledgments

We thank anonymous reviewers, the Associate Editor, and the Editor for their constructive comments. This work was supported by the Indian Council of Agricultural Research (ICAR), New Delhi, through the Challenge Research Project associated with the Lal Bahadur Shastri Young Scientist Award to the first author. We acknowledge AGU's data policy, but we do not have the ownership of the data. The rainfall and temperature data sets used in this study are obtained from Indian Meteorological Department. The other data sets are publicly available. For example, the GRACE Release 05 (RL05) gravity field solutions for TWS are available at http://grace.jpl.nasa.gov/data/get-data/ and that of the self-calibrating PDSI index at www.cgd.ucar.edu/cas/catalog/climind/pdsi.html. Moreover, the Extended Reconstructed Sea Surface Temperature Version 4 (ERSST.v4) is obtained from NOAA's official website.

References

AghaKouchak, A., L. Cheng, O. Mazdiyasni, and A. Farahmand (2014), Global warming and changes in risk of concurrent climate extremes: Insights from the 2014 California drought, *Geophys. Res. Lett.*, *41*, 8847–8852, doi:10.1002/2014GL062308.

Agricultural Statistics (2013), Government of India, Department of Agriculture and Cooperation, Directorate of Economics and Statistics, New Delhi. [Available at http://eands.dacnet.nic.in/Publication12-12-2013/AgricultralStats%20inside_website%20book.pdf.]

Alexander, L. V., et al. (2006), Global observed changes in daily climate extremes of temperature and precipitation, *J. Geophys. Res.*, *111*, D05109, doi:10.1029/2005JD006290.

Andersen, O. B., S. I. Seneviratne, J. Hinderer, and P. Viterbo (2005), GRACE-derived terrestrial waterstorage depletion associated with the 2003 European heat wave, *Geophys. Res. Lett.*, *32*, L18405, doi:10.1029/2005GL023574.

Azhar, G. S., D. Mavalankar, A. Nori-Sarma, A. Rajiva, and P. Dutta (2014), Heat-related mortality in India: Excess all-cause mortality associated with the 2010 Ahmedabad heat wave, *PLoS One*, *9*(3), e91831, doi:10.1371/journal.,pone.0091831.

Barriopedro, D., E. M. Fischer, J. Luterbacher, R. M. Trigo, and R. Garcia-Herrera (2011), The hot summer of 2010: Redrawing the temperature record map of Europe, *Science*, *332*, 220–224, doi:10.1126/science.1201224.
BBC (2003), India heat deaths exceed 1000. [Available at http://news.bbc.co.uk/2/hi/south_asia/2956490.stm.]
Berg, A., et al. (2015), Interannual coupling between summertime surface temperature and precipitation over land: Processes and implications for climate change, *J. Clim.*, *28*, 1308–1328.
Bhadram, C. V. V., B. V. S. Amatya, G. B. Pant, and K. Krishna Kumar (2005), Heat waves over Andhra Pradesh: A case study of summer 2003, *Mausam*, *56*, 385–394.
Bhat, G. S. (2006), The Indian drought of 2002 – A sub-seasonal phenomenon?, *Q. J. R. Meteorol. Soc.*, *132*, 2583–2602.
Chaudhury, S. K., J. M. Gore, and K. C. S. Ray (2000), Impact of heat waves over India, *Curr. Sci.*, *79*, 153–155.
Chen, J. L., J. Li, Z. Zhang, and S. Ni (2014), Long-term groundwater variations in Northwest India from satellite gravity measurements, *Global Planet. Change*, *116*, 130–138, doi:10.1016/j.gloplacha.2014.02.007.
Coumou, D., and S. Rahmstorf (2012), A decade of weather extremes, *Nat. Clim. Change*, *2*, 491–496, doi:10.1038/nclimate1452.
Dai, A. (2011), Characteristics and trends in various forms of the Palmer Drought Severity Index during 1900–2008, *J. Geophys. Res.*, *116*, D12115, doi:10.1029/2010JD015541.
De, U. S., and R. K. Mukhopadhyay (1998), Severe heat wave over Indian subcontinent in 1998 in a perspective of global climate, *Curr. Sci.*, *75*, 1308–1311.
De, U. S., R. K. Dube, and G. S. Prakasa Rao (2005), Extreme weather events over India in the last 100 years, *J. Indian Geophys. Union*, *9*, 173–187.
Diffenbaugh, N. S., D. L. Swain, and D. Touma (2015), Anthropogenic warming has increased drought risk in California, *Proc. Natl. Acad. Sci. U.S.A.*, *112*, 3931–3936, doi:10.1073/pnas.1422385112.
Dole, R., M. Hoerling, J. Perlwitz, J. Eischeid, P. Pegion, T. Zhang, X.-W. Quan, T. Xu, and D. Murray (2011), Was there a basis for anticipating the 2010 Russian heat wave?, *Geophys. Res. Lett.*, *38*, L06702, doi:10.1029/2010GL046582.
Donat, M. G., et al. (2013), Updated analyses of temperature and precipitation extreme indices since the beginning of the twentieth century: The HadEX2 dataset, *J. Geophys. Res. Atmos.*, *118*, 2098–2118, doi:10.1002/jgrd.50150.
Dunne, J. P., R. J. Stouffer, and J. G. John (2013), Reductions in labour capacity from heat stress under climate warming, *Nat. Clim. Change*, *3*, 563–566.
Fischer, E. M., and C. Schär (2010), Consistent geographical patterns of changes in high-impact European heatwaves, *Nat. Geosci.*, *3*, 398–403.
Fischer, E. M., S. I. Seneviratne, P. L. Vidale, D. Lüthi, and C. Schär (2007), Soil moisture–atmosphere interactions during the 2003 European summer heat wave, *J. Clim.*, *20*, 5081–5099.
Frich, P., L. V. Alexander, P. Della-Marta, B. Gleason, M. Haylock, A. Klein Tank, and T. Peterson (2002), Global changes in climatic extremes during the 2nd half of the 20th century, *Clim. Res.*, *19*, 193–212.
Gadgil, S., P. N. Vinayachandran, P. A. Francis, and S. Gadgil (2004), Extremes of the Indian summer monsoon rainfall, ENSO and equatorial Indian Ocean oscillation, *Geophys. Res. Lett.*, *31*, L12213, doi:10.1029/2004GL019733.
Government of India (2013), Census of India 2011. [Available at http://censusindia.gov.in/.]
Gupta, R., R. Gopal, M. L. Jat, R. K. Jat, H. S. Sidhu, P. S. Minhas, and R. K. Malik (2010), Wheat productivity in Indo-Gangetic plains of India: Terminal heat effects and mitigation strategies, *PACA Newslett.*, *14*, 1–11. [Available at http://www.conserveagri.org/PACA%20Newsletter%20Issue%2014.pdf.]
Hansen, J., M. Sato, and R. Ruedy (2012), Perception of climate change, *Proc. Natl. Acad. Sci. U.S.A.*, *109*(37), E2415–E2423.
Hauser, M., R. Orth, and S. I. Seneviratne (2016), Role of soil moisture versus recent climate change for the 2010 heat wave in Russia, *Geophys. Res. Lett.*, *43*, 2819–2826, doi:10.1002/2016GL068036.
Helsel, D. R., and R. M. Hirsch (2002), *Statistical Methods in Water Resources*, 524 pp., USGS Publ., Reston, Va. [Available at http://pubs.usgs.gov/twri/twri4a3/pdf/twri4a3-new.pdf.]
Hirschi, M., S. I. Seneviratne, V. Alexandrov, F. Boberg, C. Boroneant, O. B. Christensen, H. Formayer, B. Orlowsky, and P. Stepanek (2011), Observational evidence for soil moisture impact on hot extremes in southeastern Europe, *Nat. Geosci.*, *4*, 17–21, doi:10.1038/ngeo1032.
Hoerling, M., A. Kumar, R. Dole, J. W. Nielsen-Gammon, J. Eischeid, J. Perlwitz, X. Quan, T. Zhang, P. Pegion, and M. Chen (2013), Anatomy of an extreme event, *J. Clim.*, *26*, 2811–2832.
Huang, B., et al. (2015), Extended Reconstructed Sea Surface Temperature version 4 (ERSST.v4). Part I: Upgrades and intercomparison, *J. Clim.*, *28*, 911–930, doi:10.1175/JCLI-D-14-00006.1.
IMD (2014), *Annual Climate Summary 2012*, The meteorological office press, Pune, India. [Available at http://www.imdpune.gov.in/Clim_Pred_LRF_New/Reports/Annual_Climate_Summary/annual_summary_2014.pdf.]
IMD (2015), *Annual Climate Summary 2015*, The meteorological office press, Pune, India. [Available at http://www.imdpune.gov.in/Links/annual%20summary%202015.pdf.]
IPCC (2013), Summary for policymakers, in *Climate Change 2013: The Physical Science Basis. Contribution of Working Group I to the Fifth Assessment Report of the Intergovernmental Panel on Climate Change*, edited by T. F. Stocker et al., Cambridge Univ. Press, Cambridge, U. K., and New York.
Jenamani, R. K. (2012), Analysis of Ocean-Atmospheric features associated with extreme temperature variations over east coast of India- A special emphasis to Orissa heat waves of 1998 and 2005, *Mausam*, *63*, 401–422.
Karl, T. R., A. Arguez, B. Huang, J. H. Lawrimore, J. R. McMahon, M. J. Menne, T. C. Peterson, R. S. Vose, and H.-M. Zhang (2015), Possible artifacts of data biases in the recent global surface warming hiatus, *Science*, *348*, 1469–1472, doi:10.1126/science.aaa5632.
Krishna Kumar, K., K. Kamala, B. Rajagopalan, M. P. Hoerling, J. K. Eischeid, S. K. Patwardhan, G. Srinivasan, B. N. Goswami, and R. Nemani (2011), The once and future pulse of Indian monsoonal climate, *Clim. Dyn.*, *36*, 2159–2170.
Krishnamurti, T. N., A. Thomas, A. Simon, and V. Kumar (2010), Desert air incursions, an overlooked aspect, for the dry spells of the Indian summer monsoon, *J. Atmos. Sci.*, *67*, 3423–3441.
Kumari, A., and R. Maiti (2016), Climate change: Its impact on bio-resource and sustainable agriculture, in *Bioresource Stress Management*, edited by R. Maiti et al., chap. 3, pp. 13–32, Springer, Singapore.
Lau, N.-C., and M. J. Nath (2012), A model study of heat waves over North America: Meteorological aspects and projections for the twenty-first century, *J. Clim.*, *25*, 4761–4784.
Lau, W. K. M., and K.-M. Kim (2011), The 2010 Pakistan flood and Russian heat wave: Teleconnection of hydrometeorological extremes, *J. Hydrometeorol.*, *13*, 392–403.
Lesk, C., P. Rowhani, and N. Ramankutty (2016), Influence of extreme weather disasters on global crop production, *Nature*, *529*, 84–87.
Lettenmaier, D. P., E. F. Wood, and J. R. Wallis (1994), Hydro-climatological trends in the continental United States, 1948–88, *J. Clim.*, *7*, 586–607.
Lewis, S. C., and D. J. Karoly (2013), Anthropogenic contributions to Australia's record summer temperatures of 2013, *Geophys. Res. Lett.*, *40*, 3705–3709, doi:10.1002/grl.50673.

Lobell, D. B., A. Sibley, and J. I. Ortiz-Monasterio (2012), Extreme heat effects on wheat senescence in India, *Nat. Clim. Change*, *2*, 186–189.
Long, D., B. R. Scanlon, L. Longuevergne, A.-Y. Sun, D. N. Fernando, and H. Save (2013), GRACE satellites monitor large depletion in water storage in response to the 2011 drought in Texas, *Geophys. Res. Lett.*, *40*, 3395–3401, doi:10.1002/grl.50655.
Malini, B. H., K. Lalitha, M. G. Raju, and K. M. Rao (2016), Severe heat wave during May 2015 in Andhra Pradesh, *Curr. Sci.*, *110*, 1893–1894.
Mazdiyasni, O., and A. AghaKouchak (2015), Substantial increase in concurrent droughts and heatwaves in the United States, *Proc. Natl. Acad. Sci. U.S.A.*, *112*, 11,484–11,489.
Meehl, G., and C. Tebaldi (2004), More intense, more frequent, and longer lasting heat waves in the 21st century, *Science*, *305*, 994–997, doi:10.1126/science.1098704.
Met Office (2011), *Climate: Observations, Projections and Impacts: India*, Met Office, Exeter, U. K. [Available at http://www.metoffice.gov.uk/media/pdf/7/i/India.pdf.]
Miralles, D. G., M. J. van den Berg, A. J. Teuling, and R. A. M. de Jeu (2012), Soil moisture–temperature coupling: A multiscale observational analysis, *Geophys. Res. Lett.*, *39*, L21707, doi:10.1029/2012GL053703.
Miralles, D. G., A. J. Teuling, C. C. van Heerwaarden, and J. V.-G. de Arellano (2014), Mega-heatwave temperatures due to combined soil desiccation and atmospheric heat accumulation, *Nat. Geosci.*, *7*(5), 345–349, doi:10.1038/NGEO2141.
Mueller, B., and S. I. Seneviratne (2012), Hot days induced by precipitation deficits at the global scale, *Proc. Natl. Acad. Sci. U.S.A.*, *109*, 12,398–12,403, doi:10.1073/pnas.1204330109.
Murari, K. K., S. Ghosh, A. Patwardhan, E. Daly, and K. Salvi (2015), Intensification of future severe heat waves in India and their effect on heat stress and mortality, *Reg. Environ. Change*, *15*, 569–579, doi:10.1007/s10113-014-0660-6.
Nairn, J. R., and R. J. Fawcett (2014), The excess heat factor: A metric for heatwave intensity and its use in classifying heatwave severity, *Int. J. Environ. Res. Public Health*, *12*, 227–53.
Neena, J. M., E. Suhas, and B. N. Goswami (2011), Leading role of internal dynamics in the 2009 Indian summer monsoon drought, *J. Geophys. Res.*, *116*, D13103, doi:10.1029/2010JD015328.
NOAA (2015), India heat wave kills thousands. [Available at https://www.climate.gov/news-features/event-tracker/india-heat-wave-kills-thousands.]
Padmakumari, B., and B. N. Goswami (2010), Seminal role of clouds on solar dimming over the Indian monsoon region, *Geophys. Res. Lett.*, *37*, L06703, doi:10.1029/2009GL042133.
Padmakumari, B., A. K. Jaswal, and B. N. Goswami (2013), Decrease in evaporation over the Indian monsoon region: Implication on regional hydrological cycle, *Clim. Change*, *121*, 787–799, doi:10.1007/s10584-013-0957-3.
Panda, D. K., and A. Kumar (2014), The changing characteristics of monsoon rainfall in India during 1971–2005 and links with large scale circulation, *Int. J. Climatol.*, *34*, 3881–3899.
Panda, D. K., and J. Wahr (2016), Spatiotemporal evolution of water storage changes in India from the updated GRACE-derived gravity records, *Water Resour. Res.*, *52*, 135–149, doi:10.1002/2015WR017797.
Panda, D. K., A. Mishra, A. Kumar, K. G. Mandal, A. K. Thakura, and R. C. Srivastava (2014), Spatiotemporal patterns in the mean and extreme temperature indices of India, 1971–2005, *Int. J. Climatol.*, *34*, 3585–3603.
Pattanaik, D. R., M. Mohapatra, A. K. Srivastava, and A. Kumar (2016), Heat wave over India during summer 2015: An assessment of real time extended range forecast, *Meteorol. Atmos. Phys.*, doi:10.1007/s00703-016-0469-6.
Peng, S., J. Huang, J. E. Sheehy, R. C. Laza, R. M. Visperas, X. Zhong, G. S. Centeno, G. S. Khush, and K. G. Cassman (2004), Rice yields decline with higher night temperature from global warming, *Proc. Natl. Acad. Sci. U.S.A.*, *101*, 9971–9975.
Perkins, S. E., and L. V. Alexander (2013), On the measurement of heat waves, *J. Clim.*, *26*, 4500–4517.
Perkins, S. E., L. V. Alexander, and J. R. Nairn (2012), Increasing frequency, intensity and duration of observed global heatwaves and warm spells, *Geophys. Res. Lett.*, *39*, L20714, doi:10.1029/2012GL051120.
Perkins, S. E., D. Argüeso, and C. J. White (2015), Relationships between climate variability, soil moisture, and Australian heatwaves, *J. Geophys. Res. Atmos.*, *120*, 8144–8164, doi:10.1002/2015JD023592.
Prasad, A. K., and R. P. Singh (2007), Changes in aerosol parameters during major dust storm events (2001–2005) over the Indo-Gangetic Plains using AERONET and MODIS data, *J. Geophys. Res.*, *112*, D09208, doi:10.1029/2006JD007778.
Quesada, B., R. Vautard, P. Yiou, M. Hirschi, and S. I. Seneviratne (2012), Asymmetric European summer heat predictability from wet and dry southern winters and springs, *Nat. Clim. Change*, *2*(10), 736–741.
Rajeevan, M., S. Gadgil, and J. Bhate (2010), Active and break spells of the Indian summer monsoon, *J. Earth Syst. Sci.*, *119*(3), 229–247.
Ramarao, M. V. S., J. Sanjay, and R. Krishnan (2016), Modulation of summer monsoon sub-seasonal surface air temperature over India by soil moisture-temperature coupling, *Mausam*, *67*, 53–66.
Rao, B. B., P. S. Chowdary, V. M. Sandeep, V. P. Pramod, and V. U. M. Rao (2015), Spatial analysis of the sensitivity of wheat yields to temperature in India, *Agric. For. Meteorol.*, *200*, 192–202.
Rao, S. A., H. S. Chaudhari, S. Pokhrel, and B. N. Goswami (2010), Unusual central Indian drought of summer monsoon 2008: Role of southern tropical Indian Ocean warming, *J. Clim.*, *23*, 5163–5174.
Ratnam, J. V., S. K. Behera, S. B. Ratna, M. Rajeevan, and T. Yamagata (2016), Anatomy of Indian heatwaves, *Sci. Rep.*, doi:10.1038/srep24395.
Rodell, M., I. Velicogna, and J. S. Famiglietti (2009), Satellite-based estimates of groundwater depletion in India, *Nature*, *460*, 999–1002, doi:10.1038/nature08238.
Rohini, P., M. Rajeevan, and A. K. Srivastava (2016), On the variability and increasing trends of heat waves over India, *Sci. Rep.*, *6*, 26,153, doi:10.1038/srep26153.
Roxy, M. K., K. Ritika, P. Terray, R. Murtugudde, K. Ashok, and B. N. Goswami (2015), Drying of Indian subcontinent by rapid Indian Ocean warming and a weakening land-sea thermal gradient, *Nat. Commun.*, *6*, 7423.
Russo, S., A. Dosio, R. G. Graversen, J. Sillmann, H. Carrao, M. B. Dunbar, and J. V. Vogt (2014), Magnitude of extreme heat waves in present climate and their projection in a warming world, *J. Geophys. Res. Atmos.*, *119*, 12–500, doi:10.1002/2012JF002711.
Samanta, D., M. K. Dash, B. N. Goswami, and P. C. Pandey (2015), Extratropical anticyclonic Rossby wave breaking and Indian summer monsoon failure, *Clim. Dyn.*, *46*, 1547–1562.
Sen, P. K. (1968), Estimates of the regression coefficient based on Kendall's Tau, *J. Am. Stat. Assoc.*, *63*, 1379–1389, doi:10.1080/01621459.1968.10480934.
Seneviratne, S. I., M. G. Donat, B. Mueller, and L. V. Alexander (2014), No pause in the increase of hot temperature extremes, *Nat. Clim. Change*, *4*, 161–163, doi:10.1038/nclimate2145.
Sillmann, J., V. V. Kharin, F. W. Zwiers, X. Zhang, and D. Bronaugh (2013), Climate extremes indices in the CMIP5 multimodel ensemble: Part 2. Future climate projections, *J. Geophys. Res. Atmos.*, *118*, 2473–2493, doi:10.1002/jgrd.50188.

Singh, D., M. Tsiang, B. Rajaratnam, and N. S. Diffenbaugh (2014), Observed changes in extreme wet and dry spells during the south Asian summer monsoon season, *Nat. Clim. Change*, *4*, 456–461.

Sneyers, R. (1990), *On the Statistical Analysis of Series of Observations*, WMO Tech. Note 143, 192 pp., WMO, Geneva, Switzerland.

Srivastava, A. K., M. Rajeevan, and S. R. Kshirsagar (2009), Development of a high resolution daily gridded temperature data set (1969–2005) for the Indian region, *Atmos. Sci. Lett.*, *10*, 249–254, doi:10.1002/asl.232.

Stott, P. A., D. A. Stone, and M. R. Allen (2004), Human contribution to the European heatwave of 2003, *Nature*, *432*, 610–614.

Teixeira, E., G. Fischer, H. van Velthuizen, C. Walter, and F. Ewert (2013), Global hot-spots of heat stress on agricultural crops due to climate change, *Agric. For. Meteorol.*, *170*, 206–215.

Theil, H. (1950), A rank-invariant method of linear and polynomial regression analyses, I–III, *Proc. K. Ned. Akad. Wet.*, *53*, 1397–1412, doi:10.1007/978-94-011-2546-8_20.

Thomas, A. C., J. T. Reager, J. S. Famiglietti, and M. Rodell (2014), A GRACE-based water storage deficit approach for hydrological drought characterization, *Geophys. Res. Lett.*, *41*, 1537–1545, doi:10.1002/2014GL059323.

Trenberth, K. E. (2015), Has there been a hiatus?, *Science*, *349*, 691–692.

Trenberth, K. E., and J. Fasullo (2012), Climate extremes and climate change: The Russian heat wave and other climate extremes of 2010, *J. Geophys. Res.*, *117*, D17103, doi:10.1029/2012JD018020.

Trenberth, K. E., A. Dai, G. van der Schrier, P. D. Jones, J. Barichivich, K. R. Briffa, and J. Sheffield (2014), Global warming and changes in drought, *Nat. Clim. Change*, *4*, 17–22.

United Nations Economic and Social Commission for Asia and the Pacific (2016), Disasters in Asia and the Pacific: 2015 year in review. [Available at http://www.unescap.org/sites/default/files/2015_Year%20in%20Review_final_PDF_1.pdf.]

Webster, P. J., V. O. Maga'na, T. N. Palmer, J. Shukla, R. A. Tomas, M. Yanai, and T. Yasunari (1998), Monsoons: Processes, predictability and the prospects for prediction, *J. Geophys. Res.*, *103*, 14,451–14,510, doi:10.1029/97JC02719.

Westra, S., L. V. Alexander, and F. W. Zwiers (2013), Global increasing trends in annual maximum daily precipitation, *J. Clim.*, *26*, 3904–3918, doi:10.1175/jcli-d-12-00502.1.

Wilcox, R. R. (2001), *Fundamentals of Modern Statistical Methods: Substantially Improving Power and Accuracy*, Springer, New York.

Wouters, B., J. A. Bonin, D. P. Chambers, R. E. M. Riva, I. Sasgen, and J. Wahr (2014), GRACE, time-varying gravity, Earth system dynamics and climate change, *Rep. Prog. Phys.*, *77*(11), 116801, doi:10.1088/0034-4885/77/11/116801.